

# **EXPERIMENTAL AND NUMERICAL EVALUATION OF MINE PILLAR DESIGN**

A THESIS SUBMITTED IN PARTIAL FULFILLMENT OF THE  
REQUIREMENTS FOR THE DEGREE OF

**Bachelor of Technology  
in  
Mining Engineering**

By

**DEBIDAYAL MOHANTY  
109MN0479**

&

**SACHCHIDANAND SINGH  
109MN0504**



**Department of Mining Engineering  
National Institute of Technology  
Rourkela-769008  
2013**

# **EXPERIMENTAL AND NUMERICAL EVALUATION OF MINE PILLAR DESIGN**

A THESIS SUBMITTED IN PARTIAL FULFILLMENT OF THE  
REQUIREMENTS FOR THE DEGREE OF

**Bachelor of Technology  
in  
Mining Engineering**

By

**DEBIDAYAL MOHANTY  
109MN0479**

&

**SACHCHIDANAND SINGH  
109MN0504**

Under the Guidance of  
**Dr. MANOJ KUMAR MISHRA**



**Department of Mining Engineering  
National Institute of Technology  
Rourkela-769008  
2013**

**National Institute of Technology  
Rourkela**

**CERTIFICATE**

This is to certify that the thesis entitled “*EXPERIMENTAL AND NUMERICAL EVALUATION OF MINE PILLAR DESIGN*” submitted by **Mr. Debidayal Mohanty, Roll No. 109MN0479** and **Mr. Sachchidanand Singh, Roll No. 109MN0504** in partial fulfillment of the requirements for the award of Bachelor of Technology degree in Mining Engineering at the National Institute of Technology, Rourkela (Deemed University) is an authentic work carried out by them under my supervision and guidance.

To the best of my knowledge, the matter embodied in the thesis has not been submitted to any other University/Institute for the award of any Degree or Diploma.

**Date**

**(Dr. MANOJ KUMAR MISHRA)**  
**Associate Professor**  
**Department of Mining Engineering**

## **ACKNOWLEDGEMENT**

We are very much gratified to **Dr. Manoj Kumar Mishra** for allowing us to work on the topic “Experimental and Numerical evaluation of mine pillar design”. We appreciate his solemn guidance, cooperation and concern in completion of the project. With every fine effort of ours, he evinced gladness and satisfaction.

We are also thankful to **Mr. P. N. Mallick**, supporting staff, Dept. of Mining Engineering for helping & guiding me during the laboratory experiments.

We are extremely grateful to Mr. Sangram Keshari Dalai, an alumni of the department and Asst. Manager in CIL for helping us with the mine visit and data collection.

An assemblage of this nature could never have been attempted without reference to and inspiration from the works of others whose details are mentioned in reference section. I acknowledge my indebtedness to all of them.

As a final point, my sincere thanks to all my friends who have patiently extended all sorts of helps for accomplishing this assignment.

**Date**

**Debidayal Mohanty**

**Sachchidanand Singh**

Dept. of Mining Engineering

National Institute of Technology

Rourkela – 769008

# CONTENTS

	<b>Page No.</b>
CERTIFICATE	i
ACKNOWLEDGEMENT	ii
ABSTRACT	v
LIST OF FIGURES	vi
LIST OF TABLES	viii
<b>1. INTRODUCTION</b>	<b>1</b>
1.1 Background of the Problem	2
1.2 Aim and specific Objectives of the Study	2
<b>2. LITRATURE REVIEW</b>	<b>4</b>
2.1 Bord and Pillar Working Method	5
2.2 Basic Principle of Pillar Design	6
2.3 Size and Shape Effect on Compresive Strength of Pillars	10
2.3.1 Size Effect	10
2.3.2 Shape Effect	12
2.4 Pillar Strength Formulas	12
2.4.1 Obert-Duvall Formula	12
2.4.2 CMRI Formula	13
2.4.3 Bieniawski Formula	13
2.4.4 Holland - Gaddy Formula	14
2.4.5 Salamon-Munro Formula	14
2.5 Statutory Guideline	15
2.6 Effect of Mining Method of Pillar Strength	16
2.7 Factor of Safety	17
2.8 Basics of Numerical modeling	18
2.8.1 Finite Element Methods	18
2.8.2 ANSYS overview	19
<b>3. METHODOLOGY</b>	<b>21</b>
3.1 Theoretical Approach	22
3.2 Numerical Modeling approach	23
3.2.1 Steps involved in Numerical Modeling	23
<b>4. MATERIALS AND METHODS</b>	<b>26</b>
4.1 Data Collection	27
4.1.1 Sample Collection	27

4.1.2 Mining Plan and Lithology	28
4.1.3 Sample Transportation	28
4.1.4 Preparation of the Experimental Sample	28
4.2 Laboratory Tests and Analysis	29
4.2.1 Uniaxial Compressive Strength Test	29
4.2.2 Indirect Tensile Test (Brazilian test)	30
4.2.3 Triaxial Test	30
4.3 Field Data Analysis	32
4.4 Numerical Modeling	33
4.4.1 Parameters Used in Numerical Modeling	33
4.4.2 Data Used in Modeling	34
<b>5. RESULTS AND DISCUSSIONS</b>	<b>37</b>
5.1 Safety Factor Analysis	38
5.1.1 CMRI Approach (field data)	42
5.1.2 Bieniawski Approach (field data)	43
5.1.3 Obert-Duvall Approach (field data)	45
5.2 Numerical Modeling Results	46
5.2.1 Stress and Displacement Contour plot of pillar and gallery	47
5.2.2 Graphical Plot of Deformation and Stress for Result Obtained	52
5.2.2.1 Effect of Depth cover on Deformation behavior in the Pillar	52
5.2.2.2 Effect of Depth cover on Stress behavior over Pillar	52
5.2.2.3 Effect of Pillar size on Strain Developed in the Pillar	54
5.2.2.4 Effect of Gallery width on Sagging effect in the Gallery	55
5.2.2.5 Effect of Gallery width on Stress Developed over the Gallery	55
5.2.2.6 Effect of Depth cover on Sagging effect in the Gallery	57
5.2.2.7 Effect of Depth on stress Developed over the Gallery	58
<b>6. CONCLUSIONS AND RECOMMENDATION</b>	<b>61</b>
<b>REFERENCES</b>	<b>63</b>

## **ABSTRACT**

Mining is an art of extracting valuable minerals or other geological materials from the earth, usually from an ore body, vein or (coal) seam with minimum unit cost within acceptable social, legal, and regulatory constraints. There are two major methods of underground mining of coal: Bord& Pillar Method and Longwall Method. Pillars are mostly encountered in the former method. Pillar is the structural element and form an integral part of a mine on which the stability of the mine depends. A pillar support is intended to control rock mass displacement right through the zone of influence of mining, while mining activities proceeds. If pillars are made too small increasing the extraction percentage, it would affect the stability of the mine and vice-versa. An economic design of a support system implies that ore committed to pillar support be minimum, while fulfilling the vital requirements of assuring the global stability of the mine structure. This project critically studies the different optimum combination of pillar dimensions that could be effectively incorporated in the mines. Geotechnical factors of a nearby underground coal mine has been determined in the laboratory. Different approaches of pillar design have been compared. Variation of safety factors with width to height ratio of pillar, extraction percentage and depth of cover has been determined and conclusion has been made. The safety and feasibility of mining method is obtained through an optimum correlation between safety factor and extraction percentage. Numerical modeling has been done to evaluate the maximum stress induced over the pillar and gallery and also to calculate the deformation in the pillar and the sagging in gallery due to induced stress. ANSYS.13 3-D software was used in numerical modeling. Different mining parameters were changed to measure the effects on stress behavior, deformation and sagging in gallery.

## LIST OF FIGURES

Sl. No.	Name of Figures	Page No.
2.1	Schematic diagram of a typical Bord and Pillar working	6
2.2	The tributary area pillar loading concept (after, <i>Bieniawski, Z. T.</i> , 1984)	8
2.3	Compressive Strength with varying coal sample sizes	10
2.4	Finite element method showing nodes and elements	18
3.1	Flowchart of the methodology followed	22
4.1	Map showing the working area and lithology of mine area	28
4.2	Stress-strain profile of a typical coal sample	29
4.3	Failure profile observed during UCS testing	30
4.4	Mohr-coulomb criterion plot using RocData software	32
4.5	Numerical modeling with roof, pillar and floor in ANSYS	35
4.6	Numerical modeling considering the immediate roof & floor, gallery and pillar in ANSYS	36
5.1	Trend between safety factor Vs depth for different approaches	39
5.2	Relation between extraction ratio Vs depth	41
5.3	Relation between vertical stress and depths	41
5.4	Relation between w/h ratio Vs depth of the mine (CMRI Approach)	42
5.5	Relation between safety factor Vs depth of the mine (CMRI Approach)	42
5.6	Relation between extraction ratio Vs depth of the mine (CMRI Approach)	43
5.7	Relation between w/h ratio Vs depth of the mine (Bieniawski Approach)	44
5.8	Relation between safety factor Vs depth of the mine (Bieniawski Approach)	44
5.9	Relation between extraction ratio Vs depth of the mine (Bieniawski Approach)	45
5.10	Relation between w/h ratio Vs depth of the mine (Obert-Duvall Approach)	45
5.11	Relation between safety factor Vs depth of the mine (Obert-Duvall Approach)	46
5.12	Relation between extraction ratio vs depth of the mine (Obert-Duvall Approach)	46
5.13	Stress contour plot of pillar at 90 m depth of square pillar (25mx25m)	47
5.14	Deformation contour plot of pillar at 80 m Depth of square pillar (25mx25m)	48
5.15	Deformation contour plot of pillar at depth 90 m of square pillar (25mx25m)	48
5.16	Stress contour plot of gallery at depth 90 m with gallery width 4.2 m and square pillar (25 m x 25 m)	49



5.17	Deformation contour plot of gallery at depth 90 m with gallery width 3.6 m and square pillar (25 m x 25 m)	50
5.18	Stress contour plot of gallery at depth 100 m with gallery width 4 m and square pillar (25 m x 25 m)	51
5.19	Deformation contour plot of gallery at depth 100 m with gallery width 4 m	52
5.20	Depth verses deformation in pillar keeping pillar size constant (25 m X 25 m).	53
5.21	Depth verses maximum stress on the pillar keeping pillar size constant (25 m X 25 m)	54
5.22	Pillar size verses strain developed in the pillar keeping depth 90 m constant	55
5.23	Gallery width verses sagging in gallery keeping pillar size 25 m X 25 m and depth 90 m constant	56
5.24	Gallery width verses stress in gallery keeping pillar size (25 m X 25 m) and depth 90 m constant	57
5.25	Depth verses sagging in gallery keeping gallery width 4 m constant.	59
5.26	Depth verses stress in gallery keeping gallery width 4 m constant.	59

## LIST OF TABLES

<b>Sl. No.</b>	<b>Name of Tables</b>	<b>Page No.</b>
2.1	Gallery width with respect to pillar distance (centre to centre)	16
2.2	Percentage of extraction with respect to gallery width	16
4.1	Uniaxial compressive strength test result	29
4.2	Brazilian test result	30
4.3	Coal sample dimensions for Triaxial test	31
4.4	The observation obtained from Triaxial test	31
4.5	Result obtained from Triaxial test	31
4.6	Variation of pillar width with increasing depth	33
5.1	Vertical overburden stress at different depth	38
5.2	Safety factors obtained using Obert-Duvall, Bieniawski and CMRI formula	39
5.3	Variation in the extraction with increasing depth	40
5.4	Variation in vertical over-burden stress and average pillar stress with depth	40
5.5	Maximum deformation in the pillar and stress developed on the pillar with varying depth keeping other parameters constant	53
5.6	Maximum deformation and strain developed over the pillar with varying pillar size keeping other parameters constant.	54
5.7	Maximum sagging in the gallery and maximum stress induced over the gallery with varying gallery width keeping other parameter constant.	56
5.8	Maximum sagging and maximum stress developed over the gallery with varying depth cover keeping other parameters constant.	58

**CHAPTER-1**  
**INTRODUCTION**

## **1.0 Introduction**

Mining is one of the most important sectors for the progressive development or growth of any nation. Mining is the economic extraction of valuable minerals from earth for many purposes like generating power, pharmaceutical applications, infrastructures etc. It provided a base for the civilization to grow in all its form and acted as an example for the other sector of industries to breed.

Mining can be done in two ways i.e. underground and open cast. Underground mining broadly consists of two types i.e. Longwall method and Bord&Pillar method. The latter is predominantly followed in India compared to the former.

### **1.1 Background of the Problem**

Mining is one of the primitive industries that came into being since human's formative period. It provided a base for the civilization to grow in all its form and acted as an exemplar for the other sector of industries to breed.

Mining sector has always been a driving force in our country's development. Though mining has advanced leaps and bounds yet mining activities remain hazardous. Extraction of mineral wealth from underground sources is filled with many uncertainties. Underground coal mining is one such example. Still a substantial part of the coal is left to support the roof. There are many successful attempts to reduce the size of blocked coal without compromising the safety. This project is an attempt to review knowledge base available as well as evaluate the design practice of the particular nearby mine.

### **1.2 Aim and specific objectives of the study**

The purpose of the investigation is to achieve maximum production with adequate safety and optimizing the different parameters. The goal was achieved by addressing the following specific objectives.

The specific objectives of the project are

- To review current pillar design practices in terms of pillar size, pillar shape, seam thickness, depth of mining, etc.

- To study the effectiveness of Central Mining Research Institute (now CIMFR, India) pillar design formula for Underground coal pillars of Indian mines.
- To determine the safety factors as practiced elsewhere.
- To evaluate the stress induced over the pillar and the gallery and also deformation in the pillar and sagging in gallery through numerical modeling.
- To measure the effects of different mining parameters on stress, deformation and sagging.

The aim and objectives are achieved by following a scientific approach including sample collection, testing and analysis. The report incorporates all of those. Chapter one gives the background and objectives of the investigation followed by a detailed literature review in chapter two. Chapter three reflects the methodology followed with step by step approach. Chapter four describes the materials and testing processes involved whose analyses –both experimental as well as numerical, are given in chapter five including a detail discussion on the results obtained. At the end conclusions have been drawn and are given in chapter six with further suggestion.

**CHAPTER-2**  
**LITERATURE REVIEW**

## **2.0 Introduction**

Mineral wealth and its exploitation directly impart any nation's development and the standard of living of its denizens. The fossil fuel, particularly coal resources not only meets the vital energy requirement but also offers long term stability to any nation in terms of global security. Hence the exploitation of coal has been a major activity of nay nation since ages. Typically coal is mined either underground or surface method. This chapter discusses the popular method and its different aspects in detail.

### **2.1 Bord and Pillar working Method**

The Bord and Pillar method is adopted for working having characteristics such as a seam thicker than 1.5 m, a seam preferably free from stone or dirt bands. Seams at moderate depth, Seams which are not gassy, Seams with strong roof and floor which can stand for long period after development stage is over, Coal of adequate crushing strength.

Compared with the other methods of coal extraction, it offers the advantages of great operational flexibility, relative freedom in the sequence of seam extraction, insensitivity to local and regional geological disturbances, maintenance of the integrity of the roof strata and surface, and, finally, low capital intensity.

The main disadvantages of bord-and-pillar mining are that coal has to be left in situ to support the roof strata, and that the labour productivity is relatively low when compared with opencast and longwall mining systems. It is important to note that both the amount of coal being lost in the support pillars, and the labour productivity are dependent on the depth of mining.

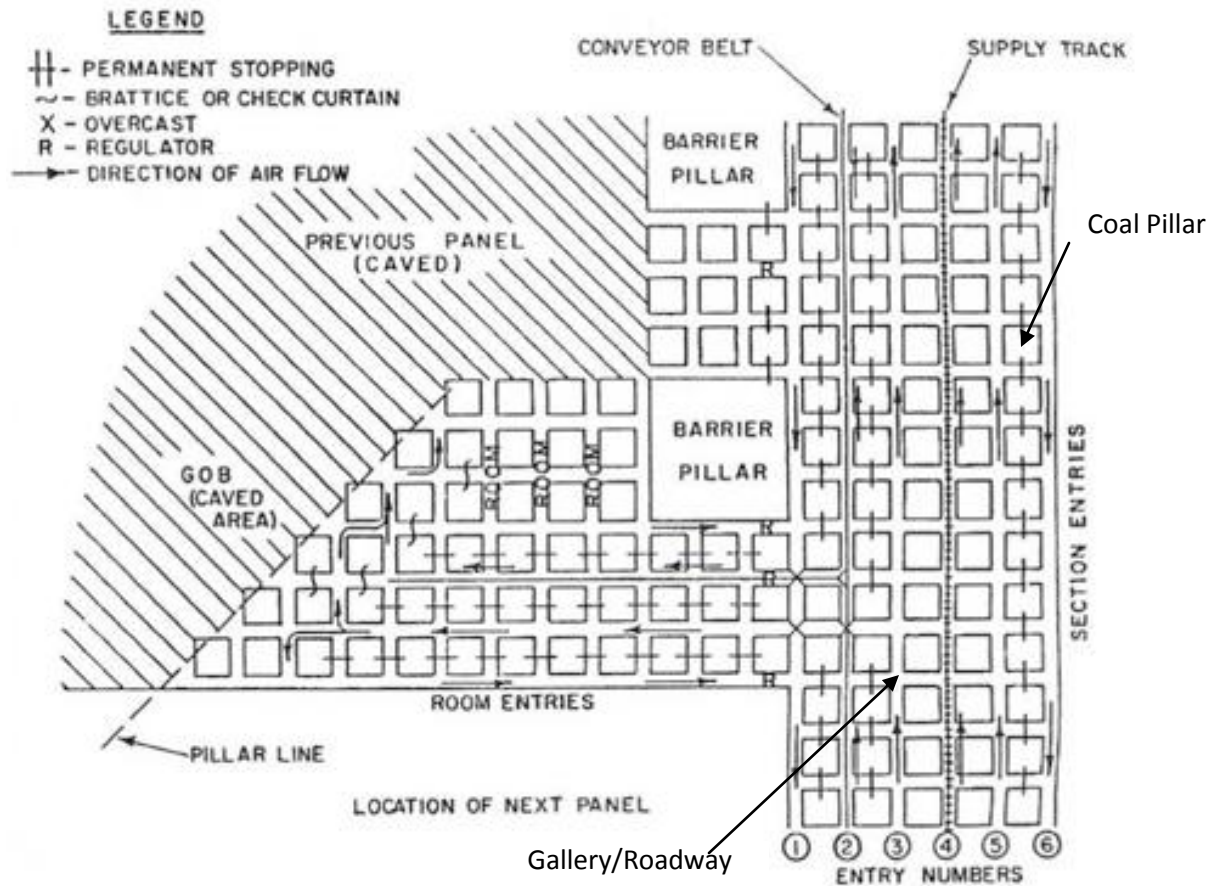


Figure 2.1: Schematic diagram of a typical Bord and Pillar working

## 2.2 Basic Principle of Pillar Design

Pillars are the natural structural member of a coal mine to support the roof and to assist in transferring the overburden load to floor for wider area dissipation. An optimum dimension/design ensures minimum coal being blocked in the pillar while maintain its stability. Nevertheless it continues to experience stresses throughout its life or till failure occurs. Pillar loading is of three types: preliminary loading or loading immediately following excavation of opening; subsequent loading or the abutment pressures (i.e. after a portion of coal has been extracted, the roof beds are detached and the beds above are relieved of the weight of the higher strata and the load which was originally acting vertically over the excavated area then deflects and bridges over the working area and transmits its weight forward to some region ahead of the coal face known as “front abutment” and backward behind the coal face at a region where the



strata again make contact by subsidence of the higher beds known as “back abutment”) and progressive failure theory for post-mining loading.

The “classic” methods consisted of three steps:

- i. Estimating the pillar load using tributary area theory;
- ii. Estimating the pillar strength using a pillar strength formula, and;
- iii. Calculating the pillar "safety factor"(SF).

Estimating the pillar load using tributary area theory:

Estimating the load was fairly straight forward for an industry that relied almost exclusively on room-and-pillar mining at relatively shallow depth. The tributary area estimate was considered sufficient, though it was recognized that in narrow panels the pillars near the edges might not experience the full load. More complex were the issues associated with pillar strength. The two big issues were the “size effect” and the “shape effect.”

According to this concept, a pillar takes the weight of overlying rock up to a distance of half the opening width surrounding it. The theory assumes that each pillar carries a proportionate share of the full overburden load.

In the figure,  $W_o$  and  $W_p$  are widths of the opening and pillar respectively, while  $L_p$  is the length of the pillar. For square pillars,  $W_p = L_p$

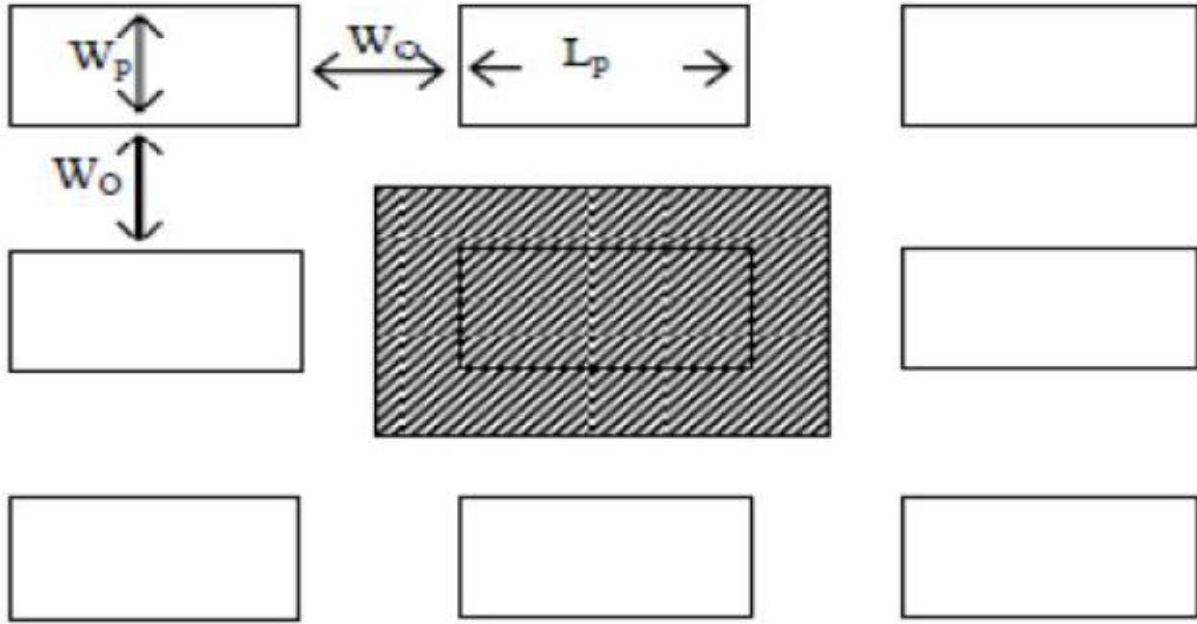


Figure 2.2: The tributary area pillar loading concept (after, Bieniawski, Z. T., 1984)

The load on the pillar, P is

$$P = (L_p + W_o) \times (W_p + W_o) * \gamma * g * h$$

Where  $\gamma * g$  is the weight of the rock per unit volume, and  $h$  is the depth of mining. The stress on the pillar  $\sigma$  is:-

$$\begin{aligned} \sigma_p &= P / \text{Area of pillar} = \frac{(L_p + W_o) \times (W_p + W_o) \times \gamma \times g \times h}{(L_p \times W_p)} \\ &= \frac{(L_p + W_o) \times (W_p + W_o) \times \sigma_v}{(L_p \times W_p)} \end{aligned}$$

In case of inclined seams the formula for stress on the pillar is

$$\sigma_p = \frac{(L_p + W_o) \times (W_p + W_o) \times \sigma_v}{(L_p \times W_p)} \times (\cos \theta + m \sin \theta)$$

Where,  $\theta$  = angle of inclination

$m$  = Poisson's ratio; and

$\sigma_v$  = vertical stress =  $\gamma gh$ .

The above equations indicate that the factors influencing pillar load are:

- Depth – the deeper the mining, the higher the load,
- Pillar width – the smaller the pillar, the higher the load,
- Bord width – the wider the bord, the higher the load, and
- Extraction ratio- The higher the extraction, the higher the pillar load.

However, a problem arises at increased depth or reduced panel widths where computer methods may be used to calculate pillar loads. If these numerically estimated loads are used in conjunction with the over-estimated strength formula, an optimistic value of the safety factor will be the result, which in turn implies that the possibility of failure will be greater than that calculated.

The pillar load is determined by using the tributary area theory, which is known to have several limitations.

**Limitations:**

- Average pillar stress is calculated by assuming that pillars uniformly support the entire load overlying both the pillars and the mined-out areas.
- Tributary area theory assumes regular geometry and ignores the presence of abutments. The effect of deformation and failure in the roof strata resulting from the mining operation are disregarded.
- The concept does not take into account abutment stress distributions and deformation or failure of the pillar. Also, if there is displacement interaction between the surrounding strata and the pillar itself, stress may be redistributed within the system, resulting in a stress state significantly different to the theoretical state (Jeremic, 1985).
- The average pillar stress is purely a convenient quantity representing the state of loading of a pillar in a direction parallel to the principal direction of confinement. It is not simply or readily related to the state of stress in a pillar that could be determined by a complete analysis of stress. The implicit assumption that the other components of the pre-mining stress field have no effect on pillar performance is not generally tenable. Furthermore the tributary area theory ignores the effect of the location of the pillar within a mine panel (Brady and Brown, 1993)

- The tributary area theory is only valid for cases where the width of the panel is as great as or greater than the depth and where the pillars in a panel are of the same size. Other factors that have been found to influence the validity of the tributary area theory include the percentage extraction and the stiffness of the overburden (Van der Merwe, 1998)

## 2.3 Size and Shape Effect on Compressive Strength of Pillars

### 2.3.1 Size effect

Compressive strength of coal depends on the distribution, type and condition of discontinuities. Smaller the specimen, less is the probability of containing discontinuities, resulting in greater strength.

The relationship between the size and the strength of the specimen can be generalized by the equation (Evans et al., 1961)

$$S_1 = k_1 d^{-\alpha}$$

Where  $S_1$  is the UCS of cubical pillars,  $d$  is the side length of the specimen and  $k_1$  and  $\alpha$  are constants.  $\alpha$  varies from 0.38 to 0.66 (Peng, 1978), with 0.5 being the average.

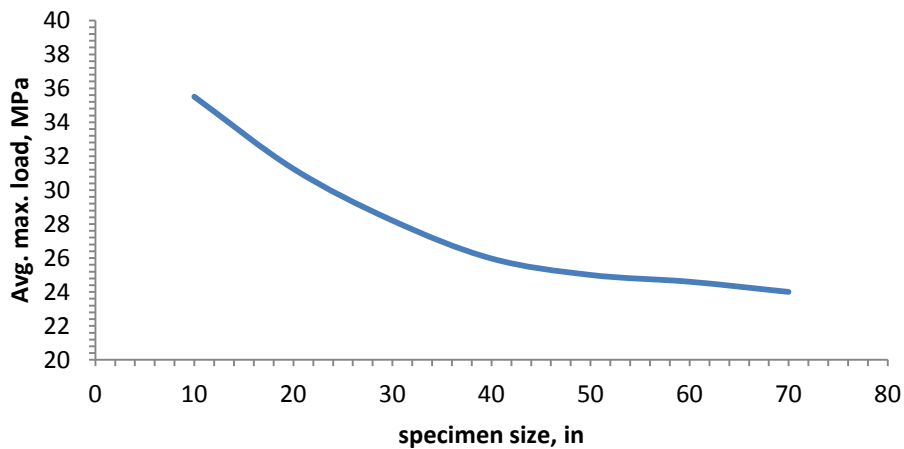


Figure 2.3: Compressive Strength with varying coal sample sizes

Bieniawski (1969) performed a series of in-situ tests and found that for cubical specimens, the strength decreases with increasing specimen size and becomes constant when it reaches the critical specimen size of approximately 5 ft for coal. This implies that the strength of the critical sample may represent the strength of the in-situ coal pillar.

Another approach for extrapolating coal strengths from the laboratory strength to the in-situ ones can be expressed by the following equations (Hustrulid, 1976):

$$S_1 = K_1/36 \quad \text{when } H \text{ is greater than } 36 \text{ in}$$

$$S_1 = K_1/\sqrt{H} \quad \text{otherwise}$$

Greenwald (1941) performed a series of experiments to determine the strength of coal pillars. The size of the cubical specimens used for the tests ranged from 1 to 60 in. the results indicated that the strength determined by the laboratory is roughly seven times the strength of the in-situ coal pillar. The same conclusion was also reached by Bieniawski and Van Heerden (1975).

Wilson (1981), suggested that the factor of strength reduction,  $F$ , from the laboratory value should depend on rock types, that is,

$F = 1$	for strong massive unjointed rock
$F = 0.5$	for widely spaced joints or bedding planes
$F = 0.33$	for more jointed but still massive rocks
$F = 0.25$	for well jointed and weaker rocks
$F = 0.20$	for coal and unstable seatearths
$F = 0.16 \text{ and } 0.14$	for fault zone

The pillars size is influenced by the following:

- Depth of cover and percentage extraction in the first workings or development.
- Strength of the coal: Seams with weak coal require large pillars. Effect of atmosphere and escape of gas also influence the size of pillars.
- The nature of the roof and floor: These influence the liability to crush and creep. A strong roof tends to crush the pillar edges whilst a soft floor predisposes it to creep and both calls for large pillars.
- Geological Considerations: In the vicinity of faults, large pillars are required. Dip and presence of water also influences the designing of pillars size.

- Time dependant strain: With time the strain goes on rising, the load remaining constant and if the size of the pillar is not sufficiently large, then it may fail under the time dependant strain, although initially it might be stable.
- Weathering takes place which decrease the strength of coal pillars with passage of time.

### 2.3.2 Shape effect

Coal strength is also found to depend on specimen geometry or shape effect i.e. the ratio of length to diameter of specimens (Evans et al., 1961; Obert and Duvall, 1967). Many formulas of average pillar strength have been proposed which can be categorised into groups:

$$S_2 = S_1 [A + B (W_p/H)]$$

$$S_2 = S_1 [W_p^a / H^b]$$

Where  $S_2$  is the pillar strength and takes into account the shape effect,  $S_1$  is the uniaxial compressive strength,  $W_p$  is the pillar width,  $H$  is the pillar height.

## 2.4 Pillar Strength Approach

Numerous pillar strength formulas have been proposed, but five formulas are used most commonly (Bieniawski, 1984; Peng, 1986). Each formula specifies its own appropriate factor of safety. These are given below:

### 2.4.1 Obert-Duvall Approach (Obert and Duvall, 1967)

It was derived from laboratory tests on hard rock and elasticity considerations the same relationship as did Bunting (1911). Greenwald et al. (1939) mention that this form of an expression for pillar strength was proposed in 1900 for anthracite after laboratory tests made for the Scranton Engineers Club. This formula is given as

$$\sigma_p = \sigma_1 (0.778 + 0.222 \frac{w}{h})$$

Where  $\sigma_p$  is pillar strength,  $\sigma_1$  is uniaxial compressive strength of a cubical specimen ( $w/h = 1$ ), and  $w$  and  $h$  are pillar dimensions in meters.

According to *Obert and Duvall*, this equation is valid for  $w/h$  ratios of 0.25 to 4.0, assuming gravity-loading conditions. Through back calculations from mining case histories and utilization of laboratory rock properties, safety factors of 2 to 4 were derived for short- and long-term pillar stability, respectively.

## 2.4.2 CMRI Approach

Central Mining Research Institute (now CIMFR, India) developed a formula for pillar strength taking into account the pillar  $w/h$  ratio, the uniaxial compressive strength of the pillar, the height of seam and depth of cover. The developed equation is nothing but a reflection of the triaxial state of different stresses involved. It is given by:

$$S = (0.27 \times \sigma_c \times h^{-0.36}) + \left[ \frac{H}{160} \left( \frac{w}{h} - 1 \right) \right]$$

Where,  $S$  = Pillar strength (in MPa)

$\sigma_c$  = Uniaxial compressive strength, UCS ( in MPa)

$h$  = Working height or seam height (in m)

$H$  = Depth of cover (in m)

$w$  = Pillar width (in m)

## 2.4.3 Bieniawski Approach

This approach is based on large-scale in situ tests on coal pillars. Such tests were first undertaken in the United States by *Greenwald et al.* (1939) during the period 1933–1941. Extensive tests were conducted in South Africa during 1965–1973 by *Bieniawski* (1968, 1969), *Wagner* (1974), and *Bieniawski and van Heerden* (1975). *Wang et al.* (1977) conducted in the United States the largest test of all involving one full-sized coal pillar measuring 80 ft (24 m) in width. All these investigations examined the various pillar-strength formulas.

The general normalize form of the Bieniawski equation is

$$\sigma_p = \sigma_1(0.64 + 0.36\frac{w}{h})$$

Where  $\sigma_p$  is pillar strength,  $w$  is pillar width (m),  $h$  is pillar height (m), and  $\sigma_1$  is the strength of a cubical specimen of critical size or greater (e.g., about 3 ft or 1 m for coal).

#### 2.4.4 Holland - Gaddy Approach

*Holland & Gaddy*, Holland (1964) extended the work by Gaddy (1956) and proposed the following formula:

$$\sigma_p = k \left( \frac{\sqrt{w}}{h} \right)$$

Where,  $k$  is the Gaddy factor,  $w$  and  $h$  are pillar dimensions in in., and  $\sigma_p$  is pillar strength in psi. Holland specified a safety factor between 1.8 and 2.2 for the design of coal pillars, with a suggested value of 2.0. The width-to height ratio, for which the Holland formula is valid, ranges from 2 to 8. Although popular in the 1970s, the Holland-Gaddy formula is no longer recommended because it was found to be overly conservative at higher ratios ( $> 5$ ).

#### 2.4.5 Salamon-Munro Approach

*Salamon and Munro* (1967) conducted a survey of failed and standing coal pillars in South Africa. Based on the studies of *Holland* (1964) and *Greenwald et al.* (1939), they selected the following form of pillar strength to apply to square pillars:

$$\text{Strength} = kh^a w^b$$

The constants for the above equation were derived from a statistical survey of data reflecting actual mining experience. In all, 125 case histories were used, of which 98 were standing pillars and 27 were failed pillars (collapsed at the time of the analysis). In deriving a pillar strength formula, it was assumed that those pillars that were still intact had safe dimensions, while the collapsed pillars were too small.



The following pillar strength formula was proposed:

$$\sigma_p = 1.32 \times \frac{w^{0.46}}{h^{0.66}}$$

Where,  $\sigma_p$  the strength is in psi, and the pillar dimensions, w and h are in feet. The recommended safety factor for this formula is 1.6, the range being 1.31 to 1.88.

In SI units, the above equation becomes:

$$\sigma_p = 7.2 \times \left( \frac{w^{0.46}}{h^{0.66}} \right)$$

Where,  $\sigma_p$  the strength is in MPa while w and h are in meters.

Based on the W/H ratio, coal pillars are divided into three categories:

- Slender pillar: pillars which have W/H ratio less than 3 or 4. When these pillars are loaded to their max. capacity, they fail completely, shedding nearly their entire load.
- Intermediate pillar: pillars which have W/H ratio in the range of 4-8. These pillars neither shed their entire load when they fail nor can accept any more load.
- Squat pillar: pillars which have W/H ratio greater than 10. These pillars can carry very large loads.

## 2.5 Statutory Guideline

In India, the dimensions of pillars and the width and height of galleries are regulated by Govt of India i.e. DGMS vide its Regulation 99 of Coal Mines Regulation 1957 (Table 2.1 & 2.2). The width of galleries should not exceed 4.8 m and the height of the galleries should not exceed 3 m. For width of galleries ranging from 3 m to 4.8 m, the dimensions of pillars for various depths of working are given below:

Table 2.1: Gallery width with respect to pillar distance (centre to centre)

Depth of the seam from the surface	Where the width of galleries does not exceed			
	3m	3.6m	4.2m	4.8m
	The distance between centres of adjacent pillars shall not be less than (in m)			
Not exceeding 60m	12	15	18	19.5
Between 60-90m	13.5	16.5	19.5	21
Between 90-150m	16.5	19.5	22.5	25.5
Between 150-240m	22.5	25.5	30.5	34.5
Between 240-360m	28.5	34	39.5	45
Exceeding 360m	39	42	45	45

It may be seen that the pillar size increases with the increase in depth as well as with the galleries. As the depth of the working increases the strata pressure increases, the rate of increase being 0.2306 kg per cm<sup>2</sup> per meter depth in Indian coalfields. Logically, therefore, to support the increased strata pressure, the size of the pillars must be increased with depth. With the increased in width of gallery, the percentage extraction is increased which in turn results in greater strata pressure per unit area of solid pillar. To counteract that, the size of the pillars again requires to be increased with the increase in the width of the galleries. Percentage extraction in development at different depths is tabulated below:

Table 2.2: Percentage of extraction with respect to gallery width

Depth of seam from surface	Where the width of galleries does not exceed			
	3 m	3.6 m	4.2 m	4.8 m
Not exceeding 60 m	43.7	42.2	41.2	43.17
Between 60-90 m	39.53	39.8	38.4	40.5
Between 90-150 m	33.06	33.5	33.8	34
Between 150-240 m	24.8	26.2	25.6	25.9
Between 240-360 m	9.95	19.7	20.1	20.2
Exceeding 360 m	14.8	16.4	17.8	19.0

## 2.6 Effect of Mining Method of Pillar Strength

The skin of the pillars is affected by blast vibrations and effect of explosion gases as they penetrate the pillars through the discontinuities. The fracturing thus caused reduces the strength of the pillar, resulting in a zone of weakness that is not present in pillars formed by continuous-miner technique. Spalling of pillars occurs resulting in the reduction of pillar width.

Salamon and Munro pillar-design formula is based on the designed mining dimensions of bord-and-pillar workings, all of which were mined by the drilling-and-blasting method, the formula for pillar strength indirectly takes into account the weakening effect of blast damages. Therefore, the effective width of a pillar designed according to the Salamon and Munro formula but mined by a continuous miner must be greater, by an amount approaching the extent of the blast zone, than that of a pillar formed by drilling and blasting.

## 2.7 Factor of Safety

Factor of Safety (SF) is the ratio of strength of pillar and stress on pillar.

$$SF = \frac{\sigma_p}{s_p} \quad \text{where } \sigma_p = \text{strength of pillar and } S_p = \text{stress on pillar}$$

The above approach of pillar design incorporates the following assumptions:

- The seam is subjected only to vertical pressure, which is constant over the mined area. However, stress transfer occurs where stiff abutments exist in underground workings. Thus this vertical pressure may be relieved partially.
- Each pillar supports the column of rock over an area that is the sum of the cross-sectional area of the pillar plus a portion of the room area, the latter being equally shared by all neighboring pillars. However, this is certainly not valid if the area of development is small since the pillars in the centre of the excavation are under more stress than the pillars close to the sides. It is usually only accepted as valid if the mined-out area is greater than the depth below surface.
- It is assumed that the load is uniformly distributed over the cross-sectional area of the pillar.

However, research has shown that:

- The stress is not evenly distributed over the cross section of an individual pillar, the maximum stress occurring at the corners formed by the intersection of three orthogonal planes, that is, two sidewalls of the pillar and the roof or the floor.
- The stress on pillars increases with percentage extraction.
- The stress distribution in pillars depends upon the ratio of pillar width to pillar height.

## 2.8 Basics of Numerical Modeling

Approach of numerical method is to divide the problem into small physical and mathematical components and then combine the all influence of the components to approximate the behavior of the whole system. The series of full mathematical equations is formed in this process then solved approximately. Various numerical modeling technique have been developed and currently being used worldwide. The methods are categorized as continuum, discontinuum and hybrid continuum or discontinuum.

The continuum postulation implies that at all point in a problem region cannot be open or broken into pieces. All material points originally in the neighborhood of a certain point in the problem region, remain in the same neighborhood throughout the deformation. The continuum problem can be solved by three different methods:

- Finite Element Method (FEM)
- Finite Difference Method (FDM)
- Boundary Element Method (BEM)

### 2.8.1 Finite Element Methods

In Finite element method structure is cuts into several elements (pieces of the structure). Then reconnect the all elements at the nodes. The behavior of each element is then defined individually using exact differential equations. The global behavior of the material is modeled by combining all individual elements.

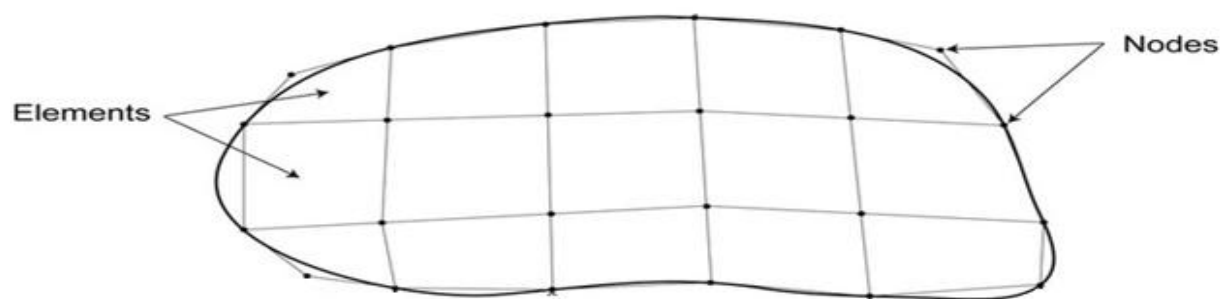


Figure 2.4: Finite element method showing nodes and elements

Finite element method is possibly the most versatile of the all methods and capable of yielding the most realistic results even in complex geo mining conditions. ANSYS is one of the software which uses the finite element techniques in numerical modeling.

A finite-element solution may be broken down into the following three stages:

**1. Preprocessing:** defining the problem

It includes the following steps (i) Define lines/area/volume (ii) Define element Type and material and geometric properties (iii) Create Geometry (iv) Mesh line/areas/volumes as required.

**2. Solution:** assigning loads, constraint and solving

Here, we have to specify the loads, constraint and finally solve the model to get the solution.

**3. Post processing:** further processing and viewing the all results.

Results includes list of nodal displacement, element force, deformation plot, stress contour diagram or temperature map.

## **2.8.2 ANSYS Overview**

ANSYS Mechanical or ANSYS Multiphysics both general-purpose finite element analysis (FEA) computer aided engineering (CAE) software tools developed by ANSYS, Inc. ANSYS is one of the leading commercial finite element programs in the world and can be applied for numerically solving the wide variety of mechanical problems. Finite element solutions are available for several engineering disciplines like statics, dynamics, heat flow, fluid flow, and electromagnetics and also coupled field problems.

There are two methods to use ANSYS. The first one is by means of graphical user interface and second one is by means of command file. Command files have the advantage that the entire analysis can be described in a small text file. This approach enables easy model modification and minimal file space requirement.

The ANSYS contains two windows: the main window and an output window, the output window displays text output from the program, such as listing of data, etc. Within the main window there are five divisions includes:

1. Utility Menu: The utility contains many functions such as file controls, selection control, graphic control and parameters.
2. Input Line: It shows program prompt message and allows to type in command directly.
3. Toolbar: The toolbar contains push buttons that execute commonly used ANSYS command.
4. Main Menu: The Main menu contains the primary ANSYS functions organized by preprocessor, solution, general postprocessor and design optimizer.
5. Graphics Window: It is where the model in its various stages of construction and the ensuing results from the analysis can be viewed.

**CHAPTER-3**  
**METHODOLOGY**

### 3.1 Theoretical Approach

The aim and specific objectives have been achieved by following a step by step scientific process as outline in figure 3.1 below.

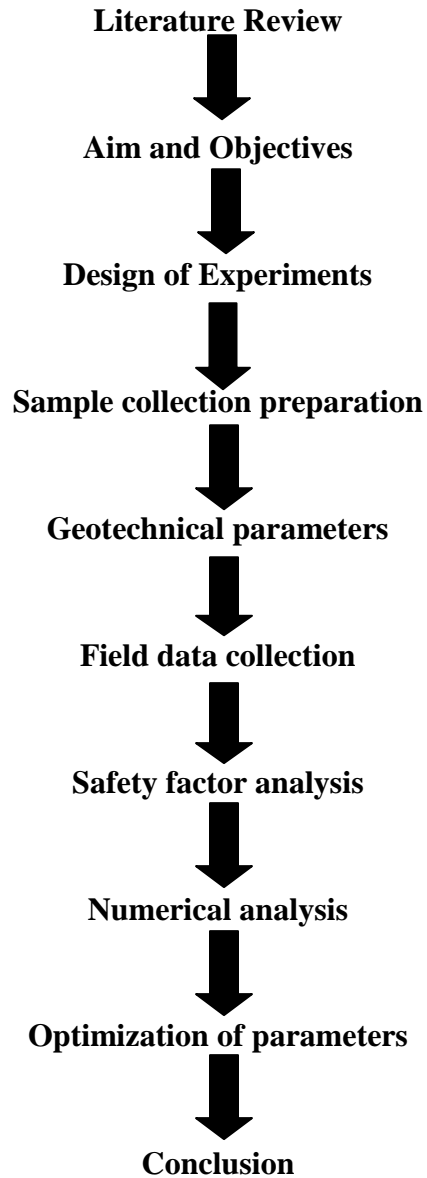


Figure 3.1: Flowchart of the methodology adopted



### **3.2 Numerical Modeling Approach**

Numerical modeling may be considered as a viable alternative method to define pillar strength. This approach will have the advantage of duly accounting for the in situ stresses as well as roof and floor strata properties. The empirical and analytical formulae do not possess this advantage. In addition, they disregard the fact that roof and floor rocks may themselves be in state of failure at the time of pillar failure (Mohan et al, 2001). Large number of parameters can be incorporated in modeling so that it will give more realistic results.

The best way for estimation of stress and strain behavior of a coal pillar is to conduct an in-situ test. In-situ test on full scale coal are very difficult, expensive and cumbersome, and also results of field and laboratory investigation are different in terms of stress-strain behavior due to inherent discontinuities within the coal mass. Hence laboratory testing for coal specimens are not suitable for determination of complete stress-strain behavior. Thus, the other methods, such as numerical methods have been evolved to analyze the pillar behavior. Numerical methods are popular and acceptable in pillar designing. They are very flexible and can quickly analyze the numerous geometric and geotechnical variable of material (Jaiswal & Shrivastva, 2008).

#### **3.2.1 Steps involved in Numerical Modeling**

These are following steps used in Numerical Modeling:

1. Defining element types and real constants
2. Defining material properties
3. Creating the model geometry
4. Meshing the model geometry
5. Applying Loads and Constraint
6. Solution
7. Analysis of results.

### **Steps 1: Defining element types and real constants**

The ANSYS element library contains more than 100 different element types. Each element type has a unique number and a prefix that identifies the element category. From **ANSYS Main Menu**, select **Preprocessor** → **ElementType** → **Add/Edit/Delete**.

### **Steps 2: Defining material properties**

Material properties are required for most element types. Depending on the application, material properties may be linear or nonlinear, isotropic, orthotropic or anisotropic, constant temperature or temperature dependent. As with element types and real constants, each set of material properties has a material reference number.

Use **ANSYS Main Menu** and select **Preprocessor** → **Material Props** → **Material Models**, Enter data characterizing the material to be used in the analysis into appropriate field. Like young modulus, poisson's ratio, density etc.

### **Step 3: Creating the model geometry**

Once material properties are defined, the next step in an analysis is to generate model geometry. Geometry may be line, area or volume. After creating model we can add or glue two models, subtract one model from the other or delete some geometry from the model.

For creating the model use ANSYS Main Menu and select-

**preprocessor** → **Modeling** → **Create** → **Line/Area/Volume** → **Create** → **Line/Area/Volume by Dimension**.

### **Step 4: Meshing the model geometry**

Mesh the whole model to create the finite element model – nodes and element adequately describing the model geometry. Use **ANSYS Main Menu** and select **Preprocessor** → **Meshing** → **Mesh Tool** → **Select Model**.

## **Step 5 Applying loads and constraint**

Load can be applied to the model in the form of force or pressure; it may be constant or varying in nature. Constraint is applied to the model to restrict the model movement. To apply the loads use

**ANSYS Main Menu and select**

**Preprocessor→Solution→Define Loads→Apply→Force/Pressure→select the Nodes, Line or Area where force or pressure to be applied→ Enter the magnitude of Force or Pressure.**

The analysis type to be used is based on the loading conditions and the response which is wished to calculate. For example, if natural frequencies and mode shapes are to be calculated, then a modal analysis ought to be chosen. The ANSYS program offers the following analysis types: static (or steady-state), transient, harmonic, modal, spectrum, buckling, and sub structuring. Not all analysis types are valid for all disciplines. In order to define the analysis type and analysis options, use **ANSYS Main Menu** and select **Main Menu: Preprocessor → Loads →Analysis Type → New Analysis.**

## **Step 6: Solution**

To initiate solution calculations, use **ANSYS Main Menu** selecting **Solution →Solve→Current LS.** After reviewing the summary information about the model, click **OK** button to start the solution. When this command is issued, the ANSYS program takes model and loading information from the database and calculates the results. Results are written to the results file and also to the database. The only dissimilarity is that only one set of results can reside in the database at one time, while a number of result sets can be written to the results file.

## **Step 7: Analysis of results.**

Once the solution has been calculated, the ANSYS postprocessors can be use to review the results. The general postprocessor is used to review results at one substep (time step) over the entire model or selected portion of the model. Using this postprocessor contour displays, deformed shapes, and tabular listing to assess and interpret the results of the analysis can be obtained

## **CHAPTER-4**

### **MATERIALS AND METHODS**

## **4.0 Introduction**

This chapter discusses about the required mine data collection and the various aspects associated with it.

### **4.1 Data Collection**

The goal and specific objectives were achieved by collecting field data as well as lab test data of the samples.

#### **4.1.1 Sample Collection**

The samples were collected from different seams at varying depths from a local underground mine colliery. The mine is located 80 kilometers from Rourkela and 30 kilometers from Talcher Road station in a lesser seismic activity zone. Seam no.1 is being mined in the mine, belongs to Karharbari measures, lower Permian period and upper Gondwana group. The over burden material consists of coarse to fine grained sandstone, carbonaceous shale, loose sand pebbles, alluvium and laterite, pink clays and pebbly sandstones, etc (Figure 4.1). The seam is almost flat having thickness of about 28 m and gradient being 1 in 20. Bord and pillar method of working was followed with conventional drilling and blasting. Ingress to the mine was via incline and coal transportation was mainly by conveyor belt. Coal samples collected were freshly exposed and undiluted coals. The samples were then placed in plastic bags and their mouths were sewed up to prevent it from exposure to moisture and atmosphere gases, so that proper condition of sample could be maintained for laboratory testing. The plastic bags were put in wooden boxes with springs inside it to prevent damage due to jerking while movement.

### 4.1.2 Mining Plan and Lithology

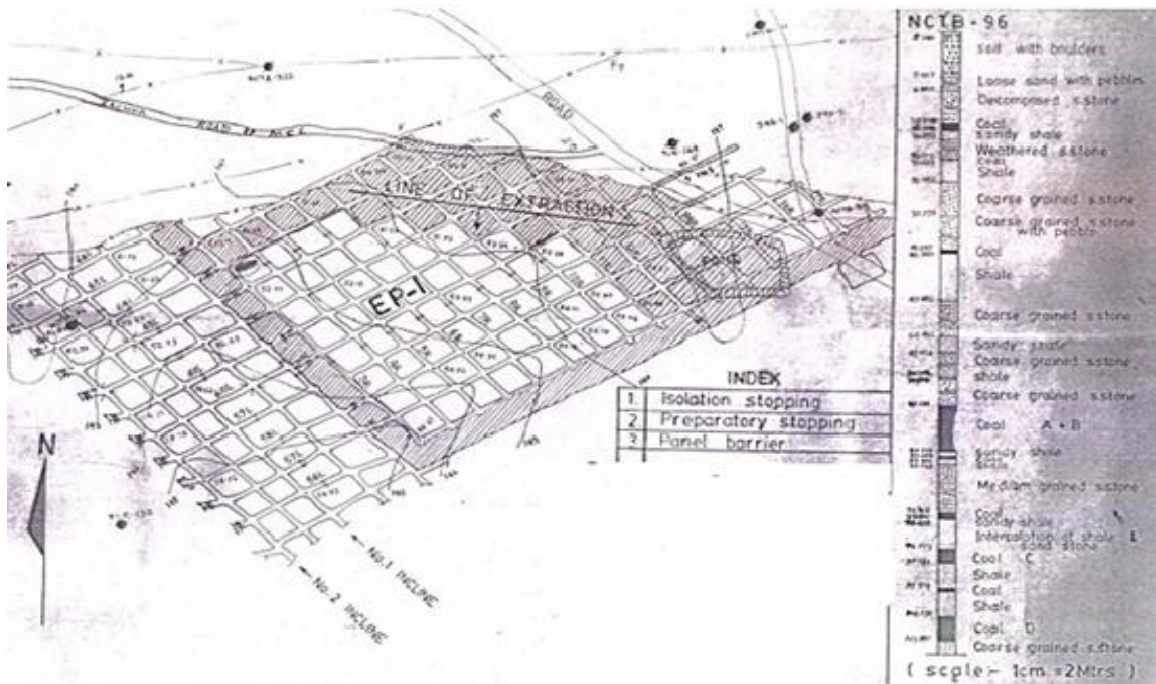


Figure 4.1: Map showing the working area and lithology of that area

### 4.1.3 Sample Transportation

The plastic bags along with the samples were transported with utmost care from the local underground colliery to the Mining Department, NIT, Rourkela through rail transport for minimum vibration.

### 4.1.4 Preparation of the Experimental Sample

Cylindrical cores of specified length to diameter ratio (kept at 2.5-3 for of UCS testing, 0.5-1.0 for tensile and 1.0-1.5 for triaxial testing) were prepared after coring (machine: make AIMIL, specification: 42 mm diamond core bit, 3 HP, 1440 rpm). The cores were finally prepared with with corundam powder for smoothness of the ends to reduce friction between platns and sanple. . These samples were then tested for uniaxial compressive strength (UCS) to find their ultimate strength and indirect tensile test for their tensile strength. Materials were also tested under Triaxial compressive testing machine so as to simulate field conditions and determine their

behavior under confined pressure as well as to determine the material properties like cohesion and friction.

## 4.2 Laboratory Tests and Analysis

### 4.2.1 Uniaxial Compressive Strength Test

The sample length used for testing was 107.5 mm and the diameter of the sample taken was 41 mm. The average UCS value of the sample was found out to be 22.7MPa. The samples took around 8 to 10 minutes to fail.

Table 4.1: Uniaxial compressive strength test results

Sl.No.	Load (KN)	$\sigma_c$ (MPa)	$\Delta l$	$\Delta d$	$\Delta l/l$	$\Delta d/d$
1	5	3.787	1.6	0.18	0.0148	0.00439
2	10	7.575	2.1	0.2	0.0195	0.00487
3	15	11.36	2.6	0.31	0.0241	0.00756
4	17	12.87	2.85	0.47	0.0265	.0114
5	20	15.15	3.1	0.59	0.0288	.0143
6	25	18.9	3.55	0.71	0.0330	.0173
7	30	22.7	3.8	0.88	0.0353	.0214

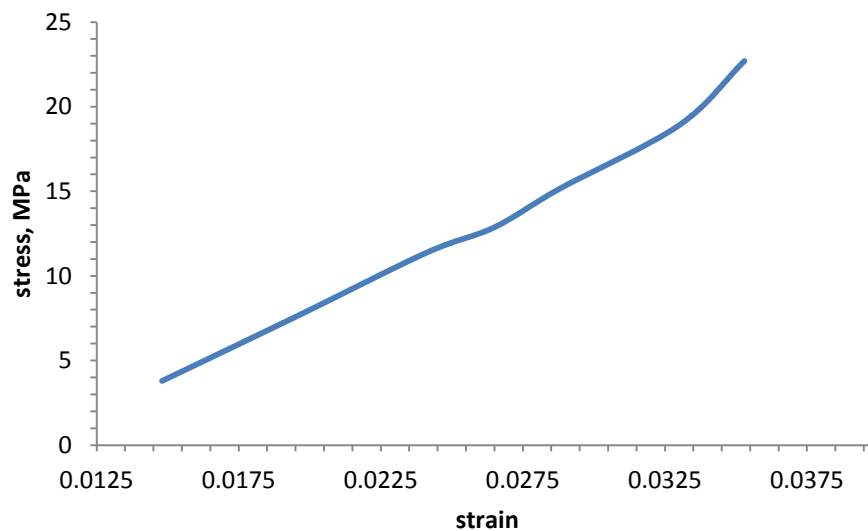


Figure 4.2: stress-strain profile of a typical coal sample



Figure 4.3: Failure profile observed during UCS testing

#### 4.2.2 Indirect Tensile Test (Brazilian test)

Two samples were used for the tensile test. The sample took around 110-130 seconds to fail. Average tensile strength was found to be 2 MPa.

Table 4.2: Brazilian test results

Sl. No.	Sample length (l)	Sample diameter (d)	l/d	Failure load (p, KN)	$\sigma_t = 2p/\pi dt$ (MPa)
1.	21mm	40 mm	0.525	2.5	1.8
2.	20 mm	41 mm	0.487	3	2.2

#### 4.2.3 Triaxial Testing

The angle of internal friction and cohesion values are typically obtained from triaxial tests. It needs at least three sets of data points. Hence two samples were used for triaxial testing and the data from compressive loading test was considered as the third set of data. The sample length and diameter used for triaxial testing are given below:



Table 4.3: Coal sample dimensions for Triaxial test

<b>Sample-1</b>	Length=54mm, Diameter= 40 mm
<b>Sample-2</b>	Length=61mm, Diameter= 40 mm

The following results were obtained:

Table 4.4: The observation obtained from Triaxial test

<b>Sample No.</b>	<b>Sample length (mm)</b>	<b>Sample diameter (mm)</b>	<b>Lateral stress (Kg/cm<sup>2</sup>)</b>	<b>Failure load (KN)</b>	<b>Vertical stress (MPa)</b>
1.	54	40	20	35	27.87
2.	61	40	40	50	39.81

The above results were used to find cohesion and angle of friction by RocData software in the following manner:

Table 4.5: Result obtained from Triaxial test

<b>Lateral stress (MPa)</b>	<b>Vertical stress (MPa)</b>
0	22.7
2.04	27.87
4.08	39.81

The following material properties were obtained using the Mohr-Coulomb criteria (Figure 4.4).

Cohesion = 1.038 MPa

Friction angle = 37.76 degrees

#### Analysis of Rock/Soil Strength using RocData

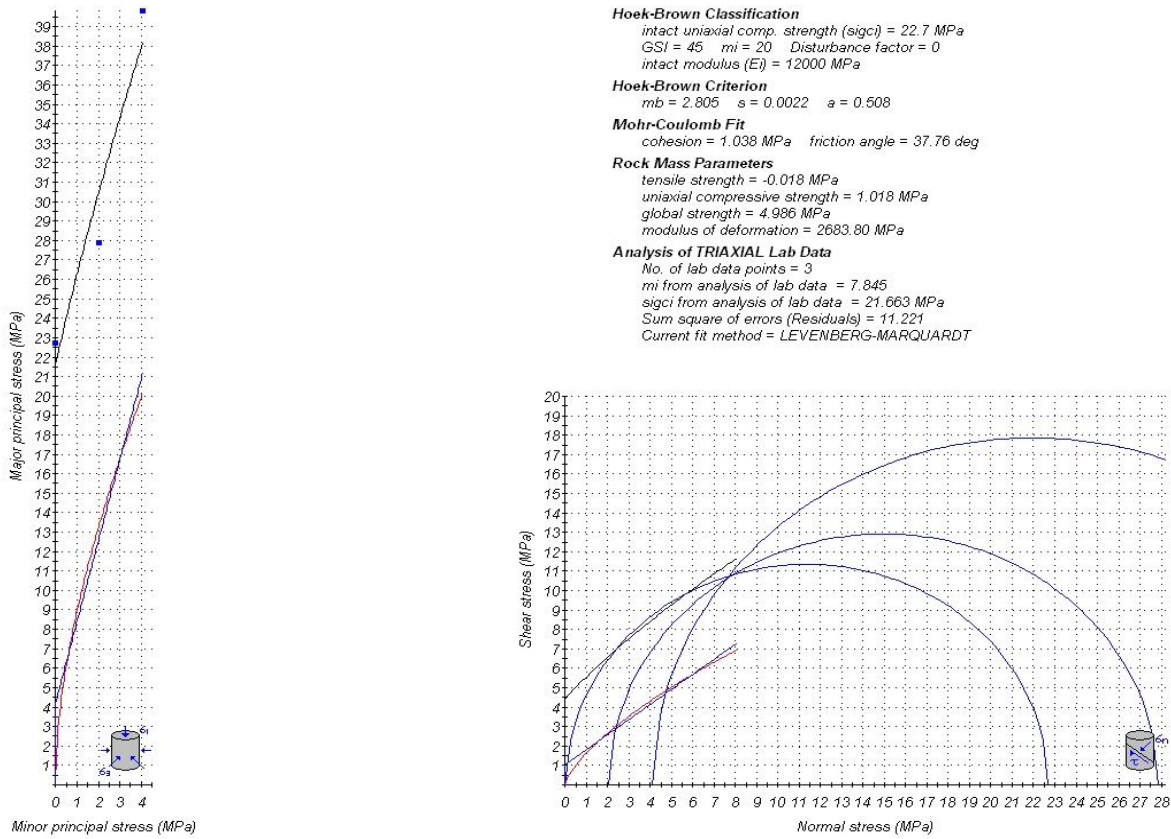


Figure 4.4: Mohr-Coulomb criterion plot using RocData software

### 4.3 Field Data Analysis

Data analysis started with visiting the mine site with designated officials from where coal samples were to be collected. Different Geotechnical parameters were studied like location of the seam, Seam thickness, Depth of the seam, Borehole data, Pillar size, Overburden density etc.

Important field data to be taken into account for pillar design:

Thickness of seam = 18 to 20 m

Working height = 2.7 m

Gradient = 1 in 30

Depth cover = 60 m to 120 m

Pillar dimension = 25 m x 25 m for seam no. 1

Gallery width = 4.0 m

Overburden specific gravity = 0.026 MPa

Variation in depth with depth as per field data:

Table 4.6: Variation of pillar width with increasing depth

Depth (m)	Pillar width (m)
60	21.1
70	21.6
80	22.2
90	22.9
100	23.7
110	24.6
120	25.6

#### 4.4 Numerical Modeling

Numerical modeling was done using ANSYS 13.0 software. The input parameter used to generate the model was taken from the site investigation and Different material properties of coal that are obtained from the laboratory data analysis.

##### 4.4.1 Parameters used in numerical model

The main sources of the input data for the numerical model are, site investigation, and laboratory and field tests. Numerical methods will give estimated solution, but not the exact solution of the problem. Following parameter is incorporated into model to generate geometric model:

- Mining Depth
- Gallery Width
- Pillar Size
- Height of pillar

By changing different parameters, one at a time and keeping others constant, different numerical model were generated and studied stress and deformation at different conditions. The parameters were changed at regular interval to get a better idea of the behaviors of the model. The parameters that were varied in the modeling were:

Pillar size: 21-25 m, the interval between variation was 1 m.

Depth of cover: 60-120 m, the interval between the variations was set at 10 m.

Gallery width: 3-4.8 m, the interval between the variation was 0.6 m.

#### 4.4.2 Data used in modeling

Material of the model was assumed to be isotropic. Model was run without considering any supports system. Depth cover varies from 60 m to 120 m. The Sandstone element was used as the depth covers and the floor material. Roof was assumed to be impermeable or very strong. The young's modulus, the poison's ratio and unit weight for the sandstone were 4 GPa, 0.30 and 26 KN/m<sup>3</sup> respectively. The properties of the coal from the experimental results are enlisted as below:

Young's modulus = 814 MPa

Poisson's ratio = 0.27

Density = 1600 Kg/m<sup>3</sup>

The bottom of the floor is constrained in moving vertically. The top of the model is left free to move in any direction. Due to non-availability of situ stress data, in-situ stress were calculated with the help of following equation:

Vertical stress =  $\gamma H$

Where,

$\gamma$  = specific weight of overlying rock mass

H = Depth cover

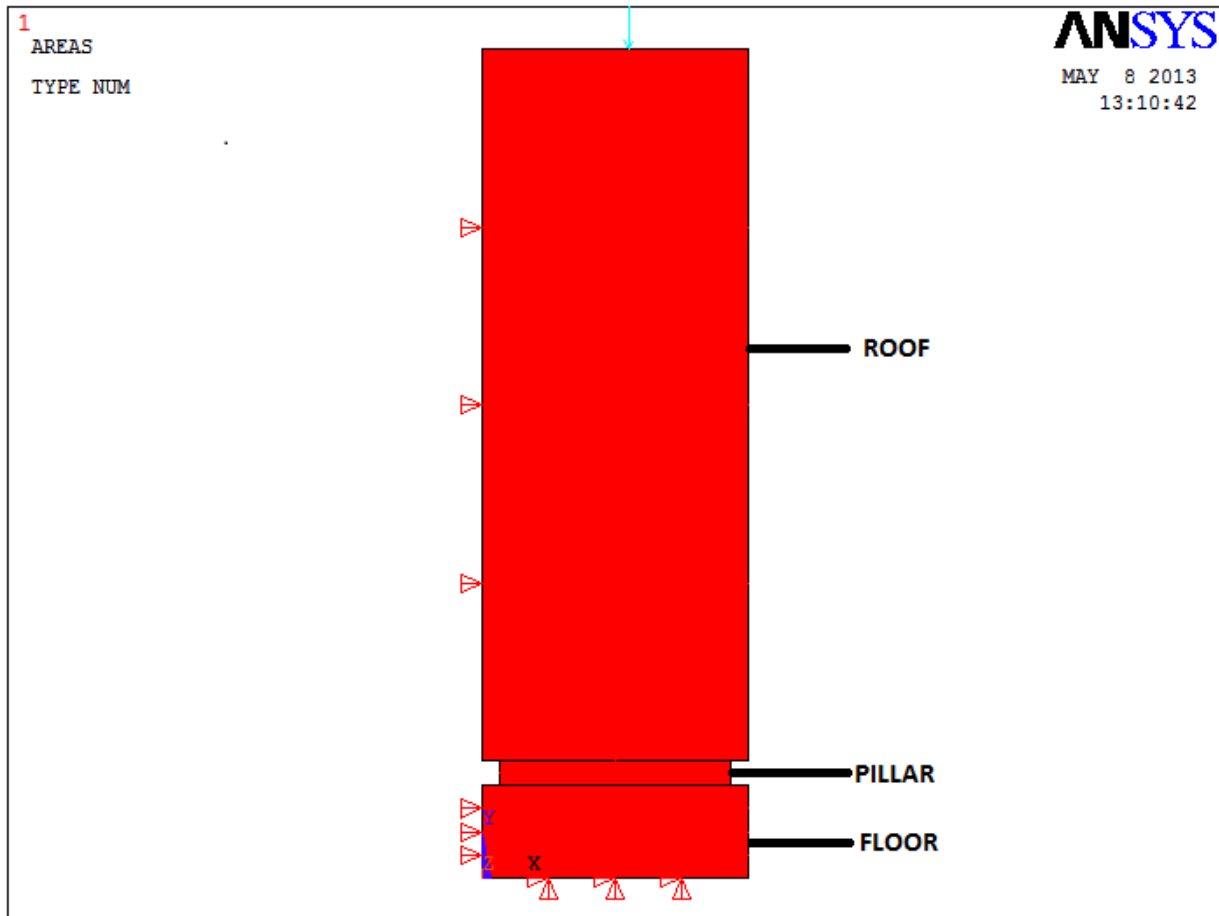


Figure 4.5: Numerical modeling with roof, pillar and floor in ANSYS

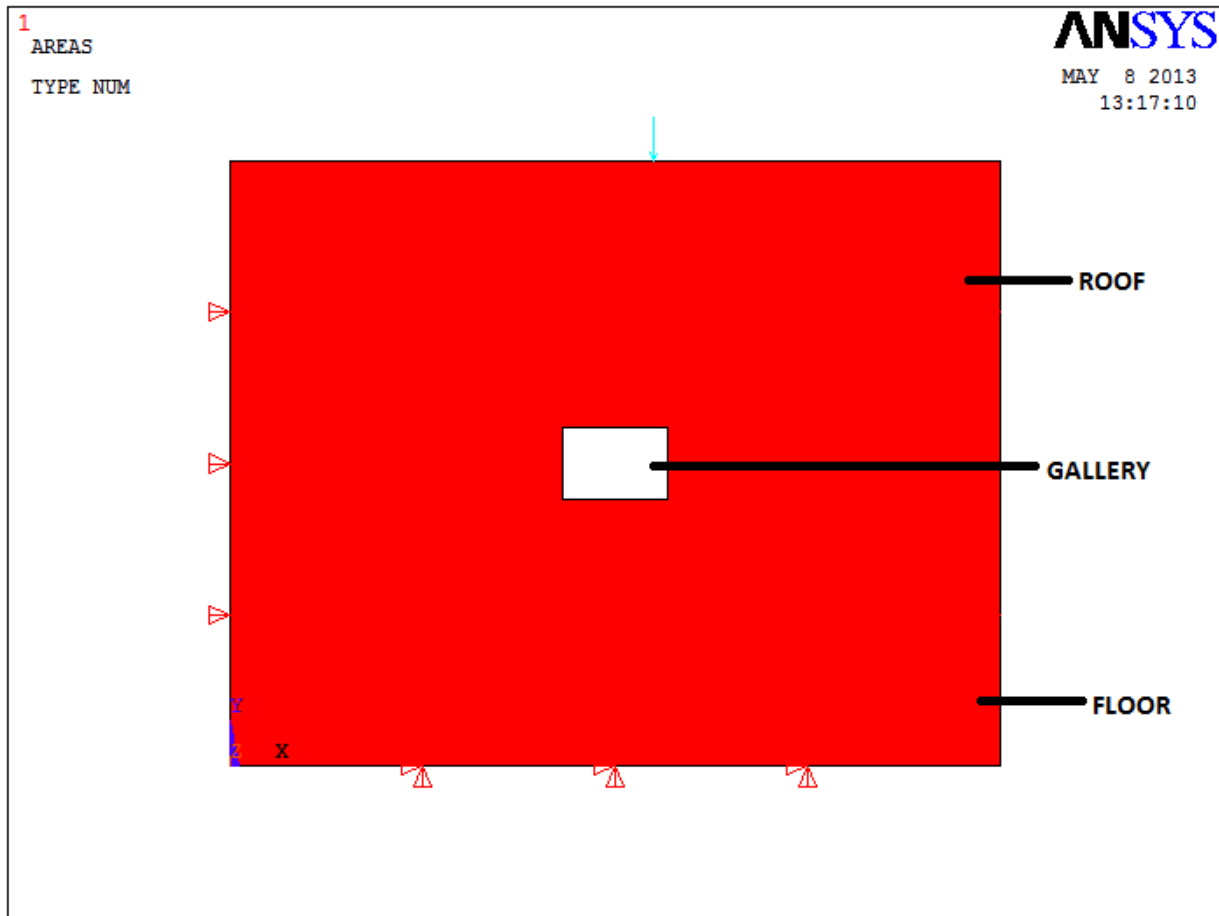


Figure 4.6: Numerical modeling considering the immediate roof & floor, gallery and pillar in ANSYS

## **CHAPTER-5**

### **RESULTS AND DISCUSSIONS**

## 5.0 Introduction

This chapter discusses the various results obtained. The safety factor calculations are done with the established approaches as Bieniawski, Obert-Duvall and CMRI (ref section 2.3.1). The different calculations are tabulated below. The field data and laboratory data analysis were used in numerical modeling.

### 5.1 Safety Factor Analysis:

The vertical overburden stress at various depths are calculated as,  $\sigma_v = \text{specific gravity} \times \text{depth}$  as shown in table 5.1.

Table 5.1: Vertical overburden stress at different depth

Depth (m)	$\sigma_v = \text{specific gravity} \times \text{depth}$	Vertical over-burden stress (MPa)
60	$0.026 \times 60$	1.56
70	$0.026 \times 70$	1.82
80	$0.026 \times 80$	2.08
90	$0.026 \times 90$	2.34
100	$0.026 \times 100$	2.6
110	$0.026 \times 110$	2.86
120	$0.026 \times 120$	3.12

Safety factors were calculated using three approaches namely Obert-Duvall, Bieniawski and CMRI. Size effect has been taken into account (Table 5.2). Working height,  $h = 2.7$  m, Gallery width = 4 m.



Table 5.2: Safety factors obtained using Obert-Duvall, Bieniawski and CMRI formula

				<b>Obert-Duvall approach</b>		<b>Bieniawski approach</b>		<b>CMRI approach</b>	
<b>Depth (m)</b>	<b>Width of pillar (m)</b>	<b>w/h ratio</b>	<b>Avg. pillar stress (MPa)</b>	<b>Pillar strength (MPa)</b>	<b>Safety factor</b>	<b>Pillar strength (MPa)</b>	<b>Safety factor</b>	<b>Pillar strength (MPa)</b>	<b>Safety factor</b>
60	21.1	7.81	2.207	6.0	2.72	8.249	3.737	6.84	3.1
70	21.6	8	2.556	6.104	2.388	8.413	3.291	7.348	2.87
80	22.2	8.22	2.897	6.220	2.147	8.602	2.969	7.897	2.725
90	22.9	8.48	3.228	6.359	1.969	8.825	2.733	8.494	2.63
100	23.7	8.77	3.551	6.512	1.833	9.075	2.555	9.147	2.575
110	24.6	9.11	3.865	6.693	1.731	9.367	2.423	9.862	2.55
120	25.6	9.48	4.171	6.889	1.651	9.686	2.322	10.647	2.54

Safety factor is obtained by dividing pillar strength with average pillar stress. Maximum safety factor in all the three approaches has been observed at 60 m and decreases gradually with increasing depth.

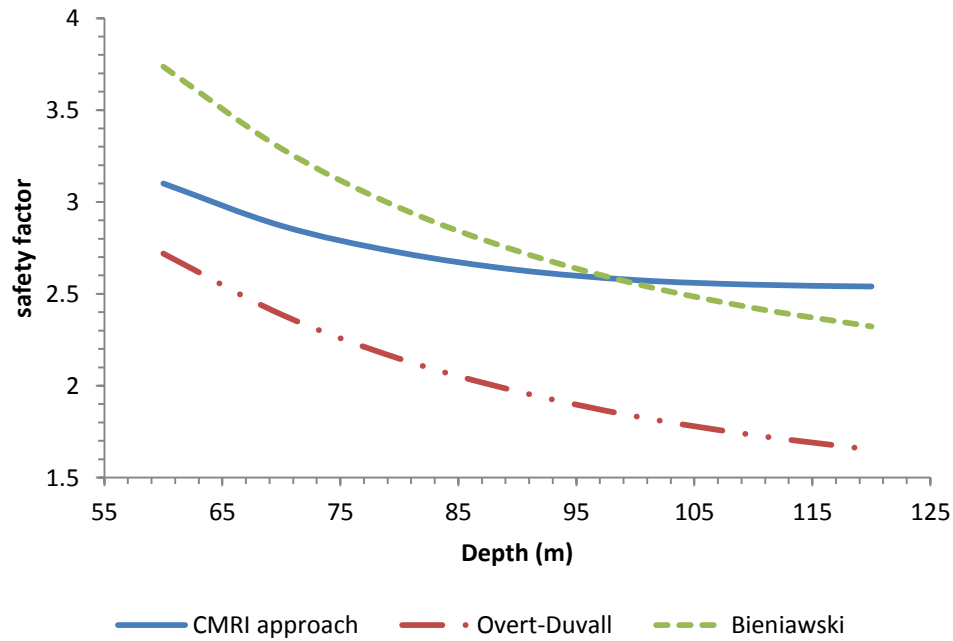


Figure 5.1: Trend between safety factor Vs depth for different approaches

As observed from the above graph (figure 5.1), safety factor decreases with increase in depth in Bieniawski, Obert-Duvall and CMRI approach.

Extraction percentage depends only on the geometrical dimension of the pillars and is independent of the various formulas used in Obert-Duvall, Bieniawski and CMRI approaches (table 5.3).

Table 5.3: Variation in the extraction with increasing depth

<b>Depth (m)</b>	<b>Extraction ratio (%)</b>
60	29.3
70	28.8
80	28.2
90	27.5
100	26.8
110	26
120	25.2

Average pillar stress increases with increasing depth.

Table 5.4: Variation in vertical over-burden stress and average pillar stress with depth

<b>Depth (m)</b>	<b>Vertical over-burden stress (MPa)</b>	<b>Avg. pillar stress (MPa)</b>	<b>Extraction ratio (%)</b>
60	1.56	2.207	29.3
70	1.82	2.556	28.8
80	2.08	2.897	28.2
90	2.34	3.228	27.5
100	2.6	3.551	26.8
110	2.86	3.865	26
120	3.12	4.171	25.2

With increase in depth, extraction ratio decreases from 29.3 to 25.2 (figure 5.2) and vertical stress increases with increase in depth (figure 5.3).

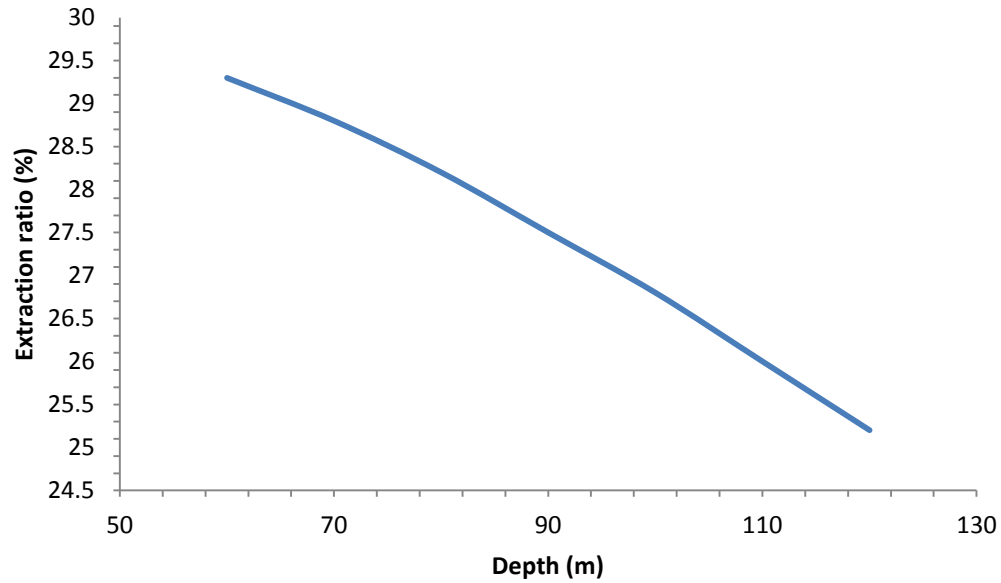


Figure 5.2: Relation between extraction ratio Vs depth

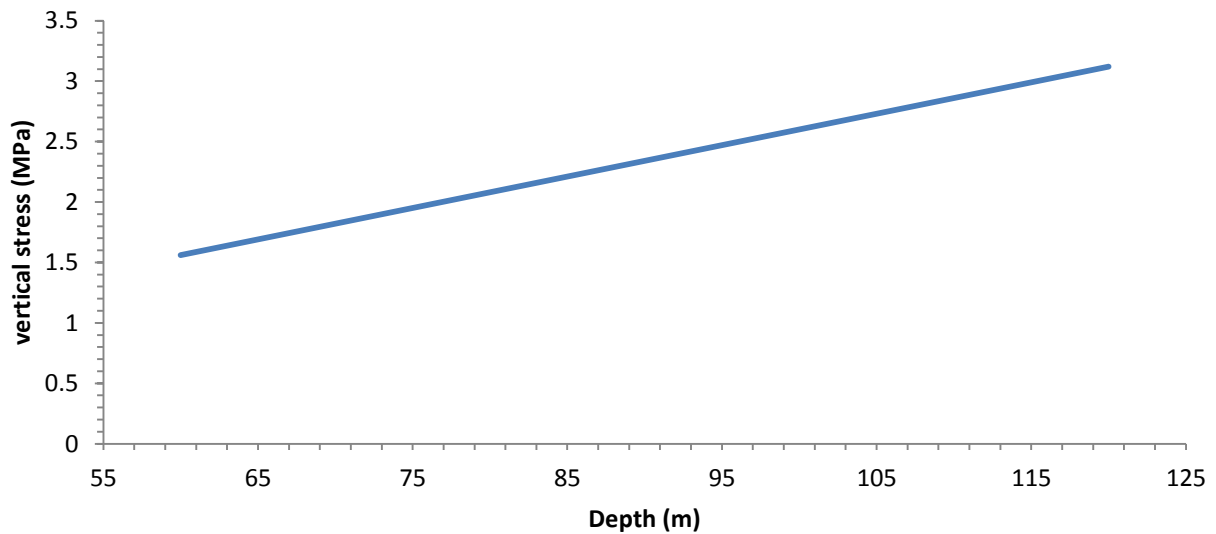


Figure 5.3: Relation between vertical stress and depths

The following graphs were obtained using Obert-Duvall, Bieniawski and CMRI formula for pillar design by putting the values in the respective formulas specified in Table 5.2.

### 5.1.1 CMRI Approach (field data):

The CMRI approach shows that as the mining depth increases there is a decreasing trend in the extraction ratio because of large size pillars left to support the roof. The rate of increase is almost linear for the w/h ratio and linearly decreases extraction percentage (Figure 5.4 & 5.5). The w/h ratio ranges from 7.81 to 9.48, the extraction percentage varies from 29.3 to 25.2 and the safety factor decreases moderately from 3.1 to 2.54 (Figure 5.5).

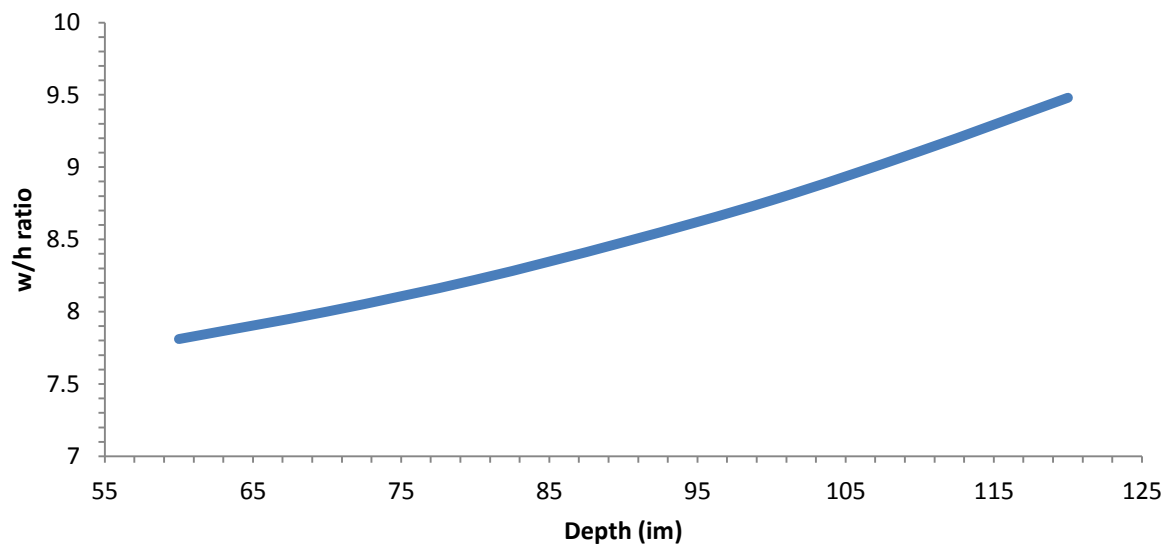


Figure 5.4: Relation between w/h ratio Vs depth of the mine

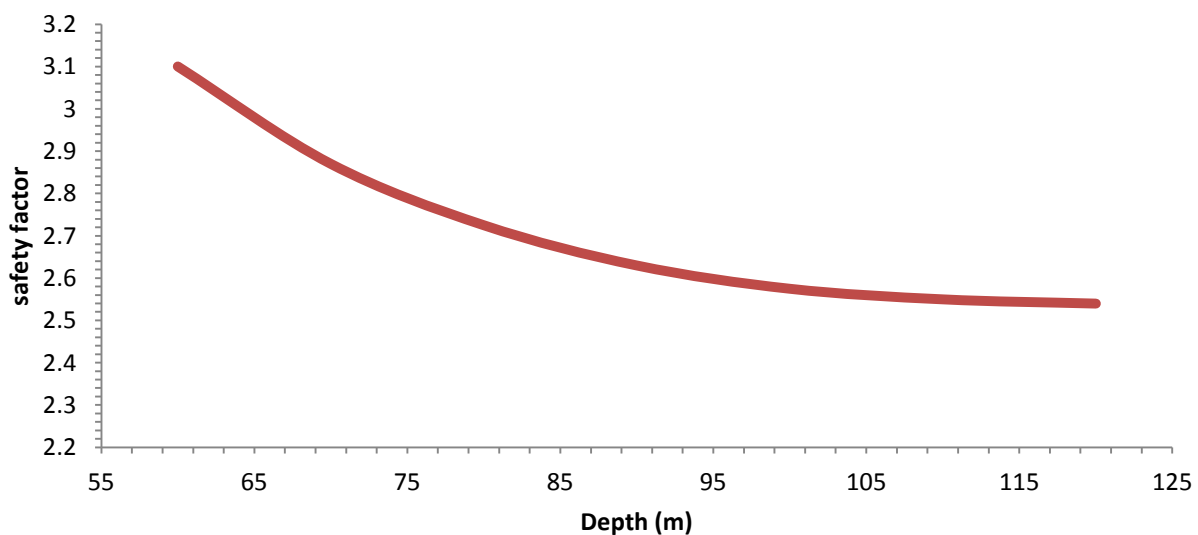


Figure 5.5: Relation between safety factor Vs depth of the mine

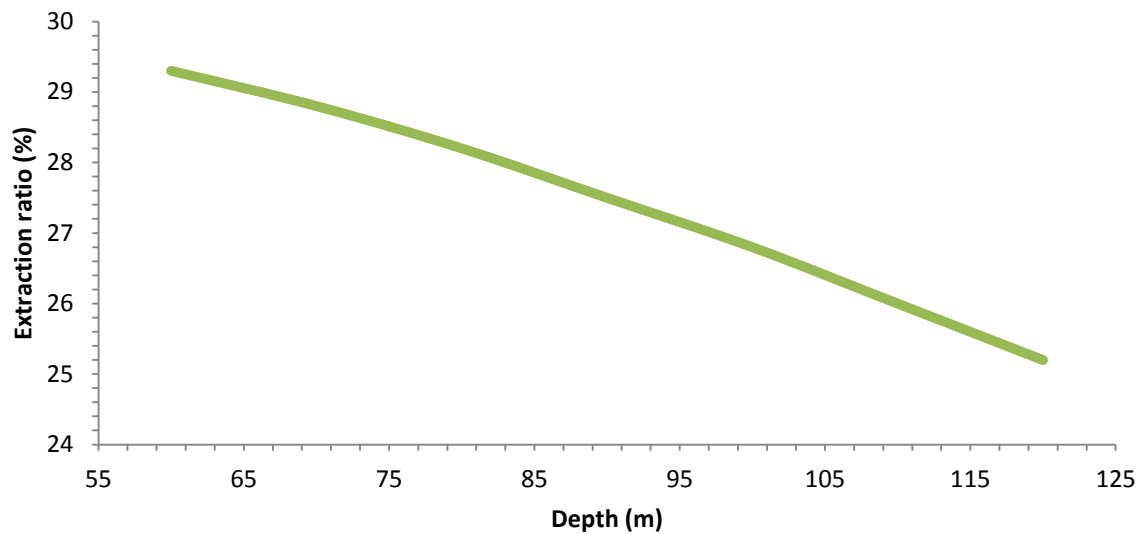


Figure 5.6: Relation between extraction ratio Vs depth of the mine

### 5.1.2 Bieniawski Approach (field data):

The Bieniawski approach shows that as the mining depth increases there is a decreasing trend in the extraction ratio because of large size pillars left to support the roof. The rate of increase is almost linear for the w/h ratio and linearly decreases extraction percentage (Figure 5.7& 5.8). The w/h ratio ranges from 7.81 to 9.48, the extraction percentage varies from 29.3 to 25.2 and the safety factor decreases moderately from 3.7 to 2.3 (Figure 5.9).

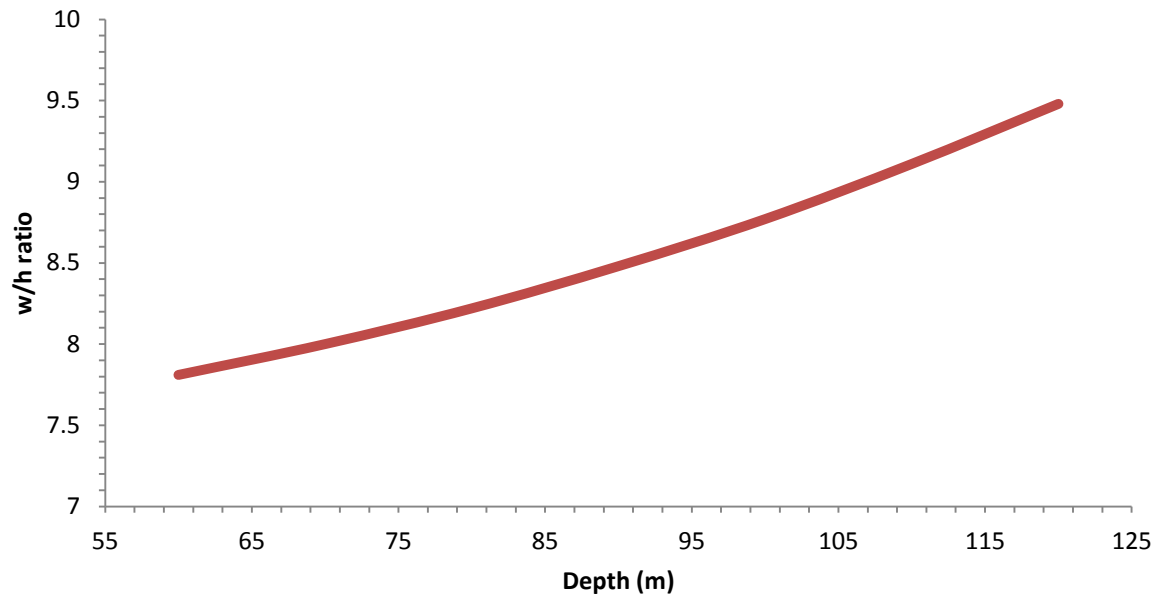


Figure 5.7: Relation between w/h ratio Vs depth of the mine

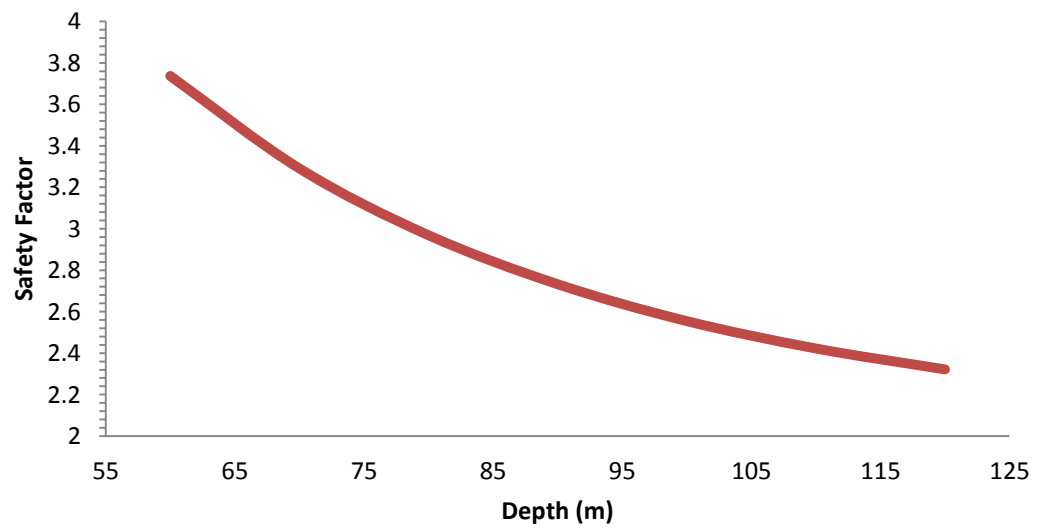


Figure 5.8: Relation between safety factor Vs depth of the mine

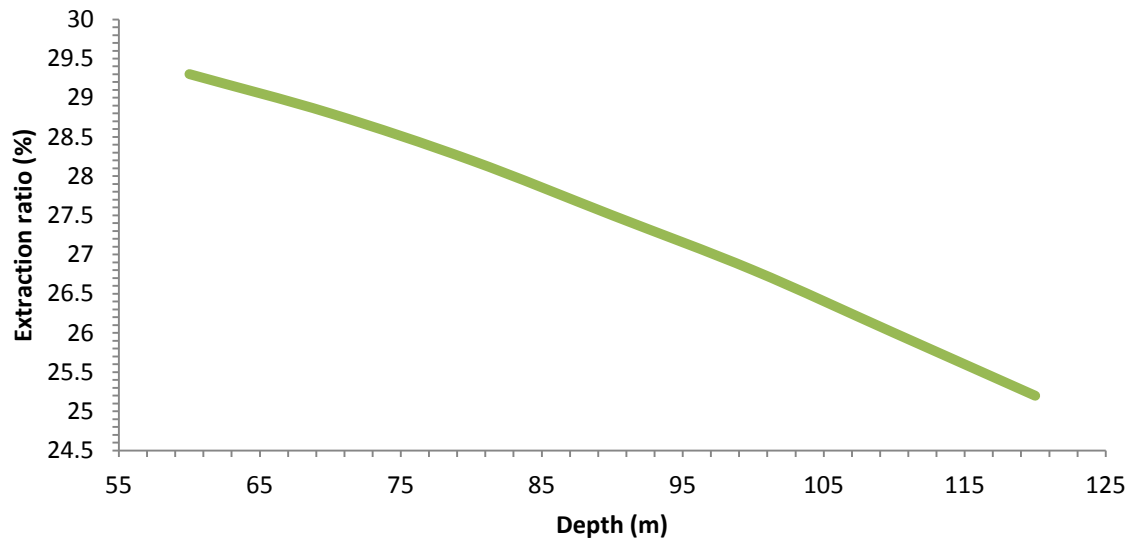


Figure 5.9: Relation between extraction ratio Vs depth of the mine

### 5.1.3 Obert-Duvall Approach (field data):

The Obert-Duvall approach shows that as the mining depth increases there is a decreasing trend in the extraction ratio because of large size pillars left to support the roof. The rate of increase is almost linear for the  $w/h$  ratio and linearly decreases extraction percentage (Figure 5.10 & 5.11). The  $w/h$  ratio ranges from 7.81 to 9.48, the extraction percentage varies from 29.3 to 25.2 and the safety factor decreases moderately from 2.7 to 1.6 (Figure 5.12).

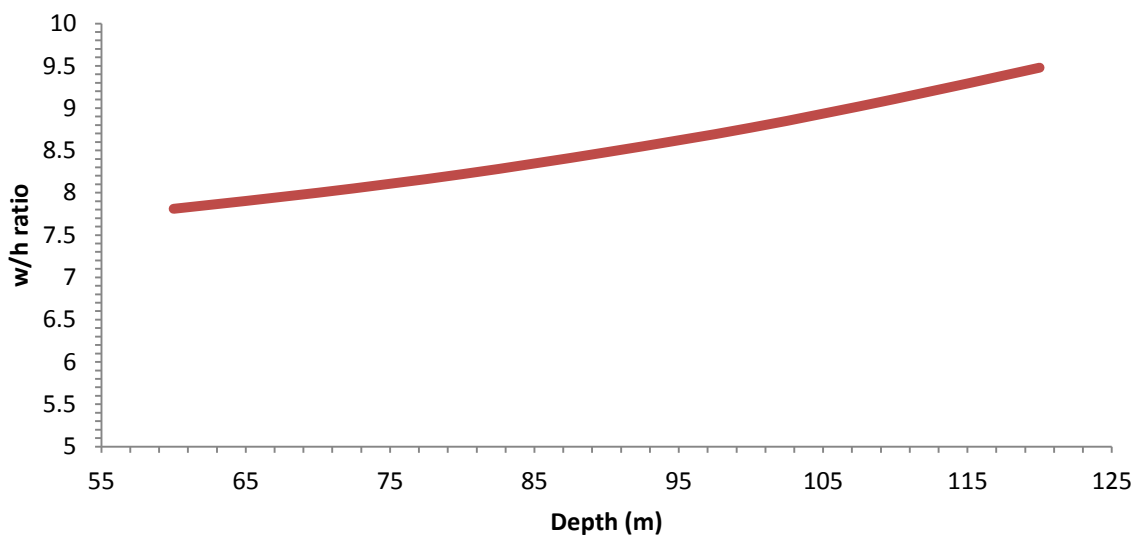


Figure 5.10: Relation between  $w/h$  ratio Vs depth of the mine

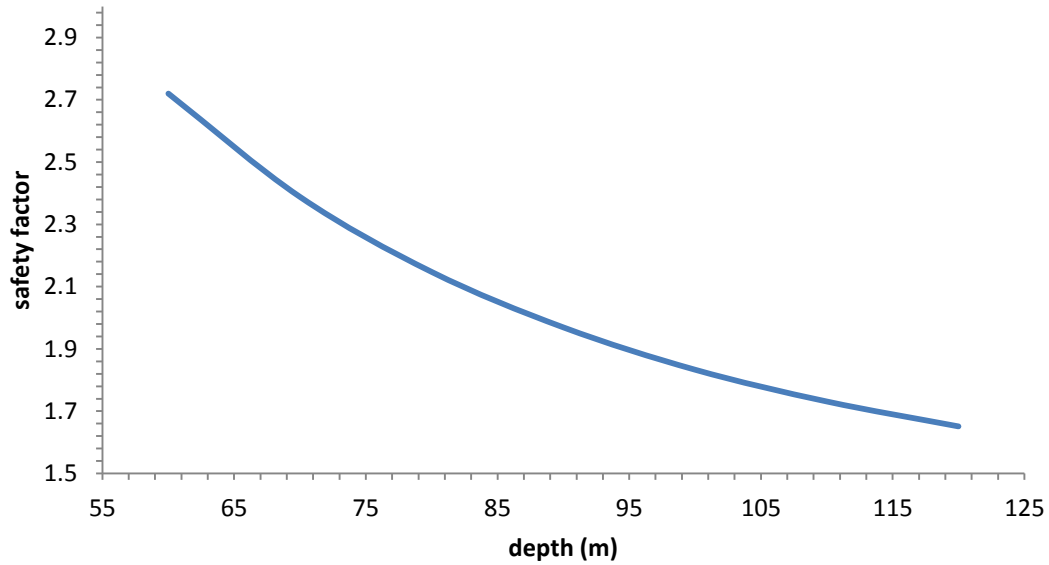


Figure 5.11: Relation between safety factor Vs depth of the mine

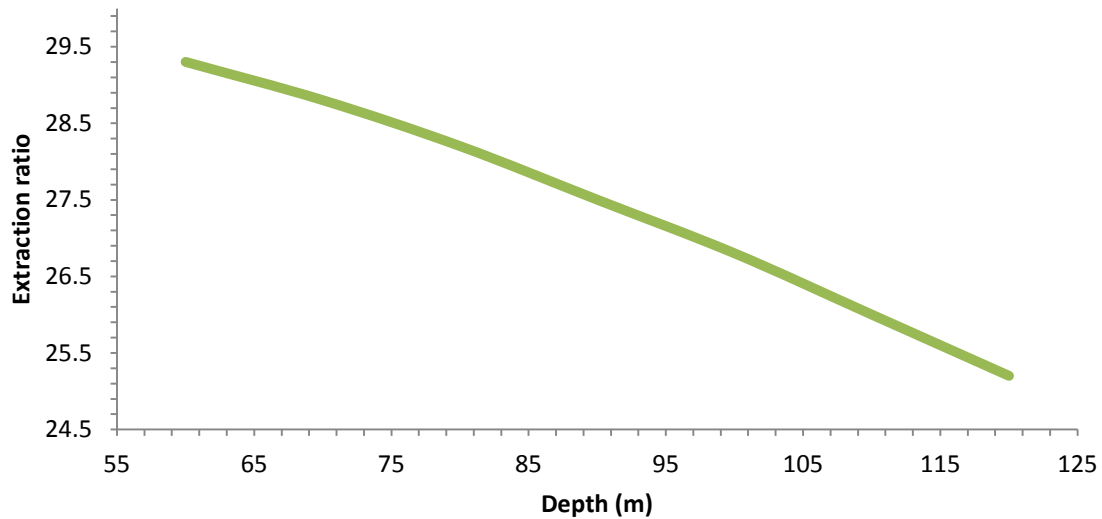


Figure 5.12: Relation between extraction ratio Vs depth of the mine

## 5.2 Numerical Modeling Results

Numerical modeling was done to evaluate the stress over the pillar and deformation in the pillar by varying various mining parameters. Only one parameter was changed at a time and keeping other parameters constant. Sagging effect in the gallery and the stress over the gallery was also estimated with varying gallery width and depth cover. For this purpose seven depths were



considered (60 m, 70 m, 80 m, 90 m, 100 m, 110 m, and 120 m). Pillar sizes were also varied (21 m to 25 m with difference of 1 m) to calculate the strain developed over the pillar. Gallery width was varied (3 m, 3.6 m, 4.2 m, 4.8 m) to estimate the sagging in gallery. Overall 20 different models were run for this purpose. Finite element method was used for the study. The software used was 3-Dimensional ANSYS 13.0

### 5.2.1 Stress and Displacement Contour plot of Pillar and gallery of some typical Condition

1. Stress contour plot of pillar at 90 m depth of square pillar (25 m x 25 m), height 2.75 m. maximum stress over the pillar at corners was found to be 2.42 MPa (figure 5.13).

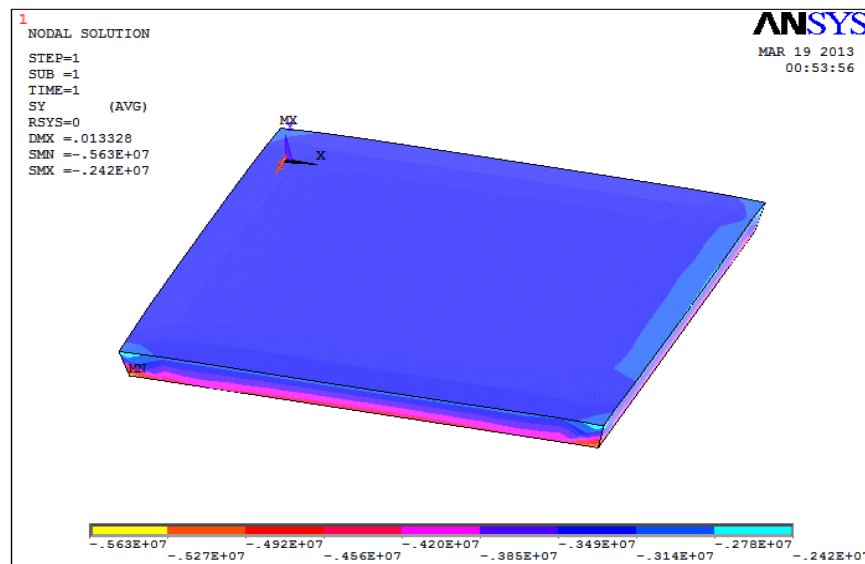


Figure 5.13: Stress contour plot of pillar at 90 m depth of square pillar (25 m x 25 m).

2. Deformation contour plot of pillar at 80 m depth of square pillar (25 m x 25 m) and height 2.7m. Maximum deformation was 0.011 m (or 1.1 cm). Figure 5.14 shows that maximum deformation is at edges of the pillar and the minimum deformation experienced by central portion of the pillar.

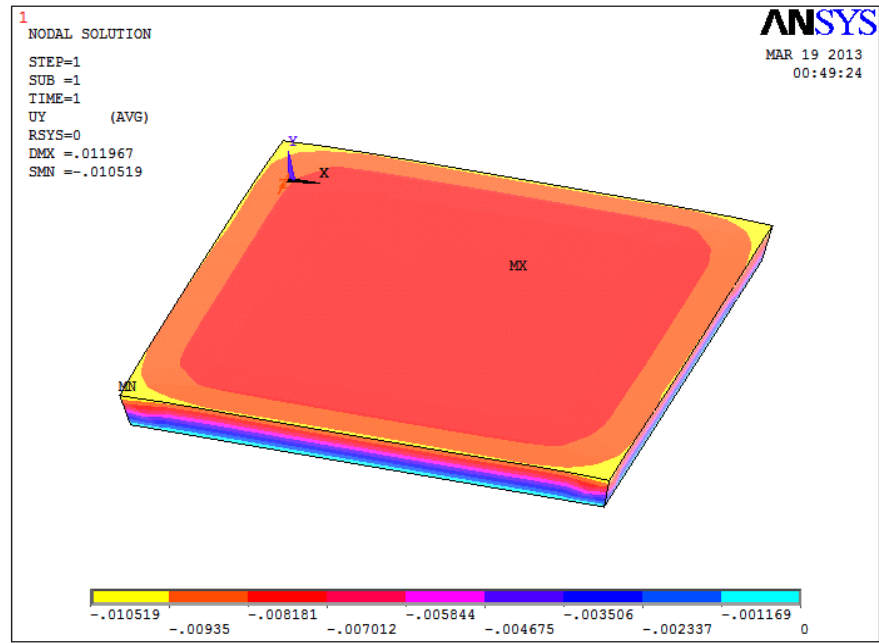


Figure 5.14: Deformation contour plot of pillar at 80 m depth of square pillar (25 m x 25 m).

3. Deformation contour plot of pillar at depth 90 m of square pillar (25 m x 25 m), height 2.7 m and gallery width 4 m. Maximum deformation developed in the pillar (figure 5.15) was 0.0546 m (or 5.4 cm).

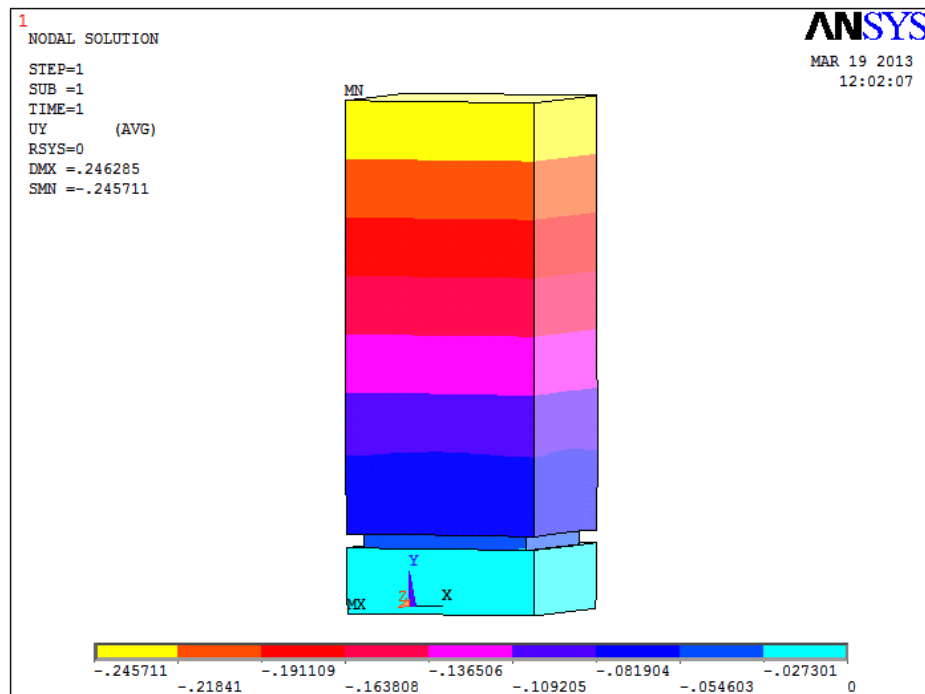


Figure 5.15: Deformation contour plot of pillar at depth 90 m of square pillar (25 m x 25 m).

4. Stress contour plot of gallery at depth 90 m with gallery width 4.2 m, square pillar (25 m x 25 m) and pillar height 2.7 m. Maximum stress induced observed over the gallery was 3.39 MPa (figure 5.16).

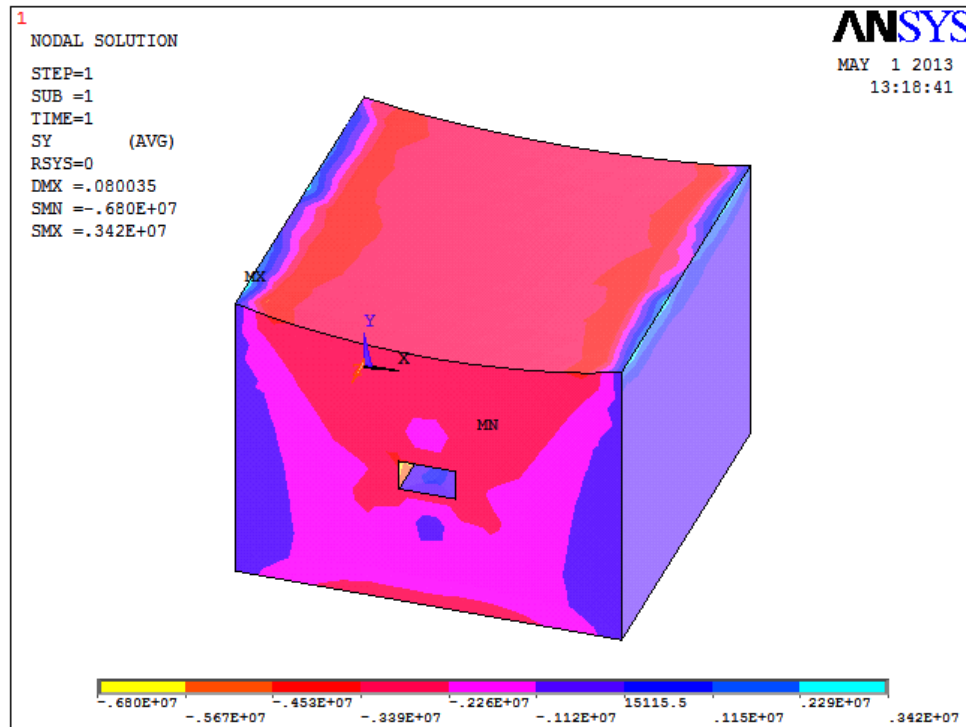


Figure 5.16: Stress contour plot of gallery at Depth 90 m with gallery width 4.2 m, square pillar (25 m x 25 m)

5. Deformation contour plot of gallery at Depth 90 m with gallery width 3.6 m, Square Pillar (25 m x 25 m), pillar height 2.7 m (figure 5.17).Maximum sagging observed in this case was 0.077 m (or 7.7 cm).

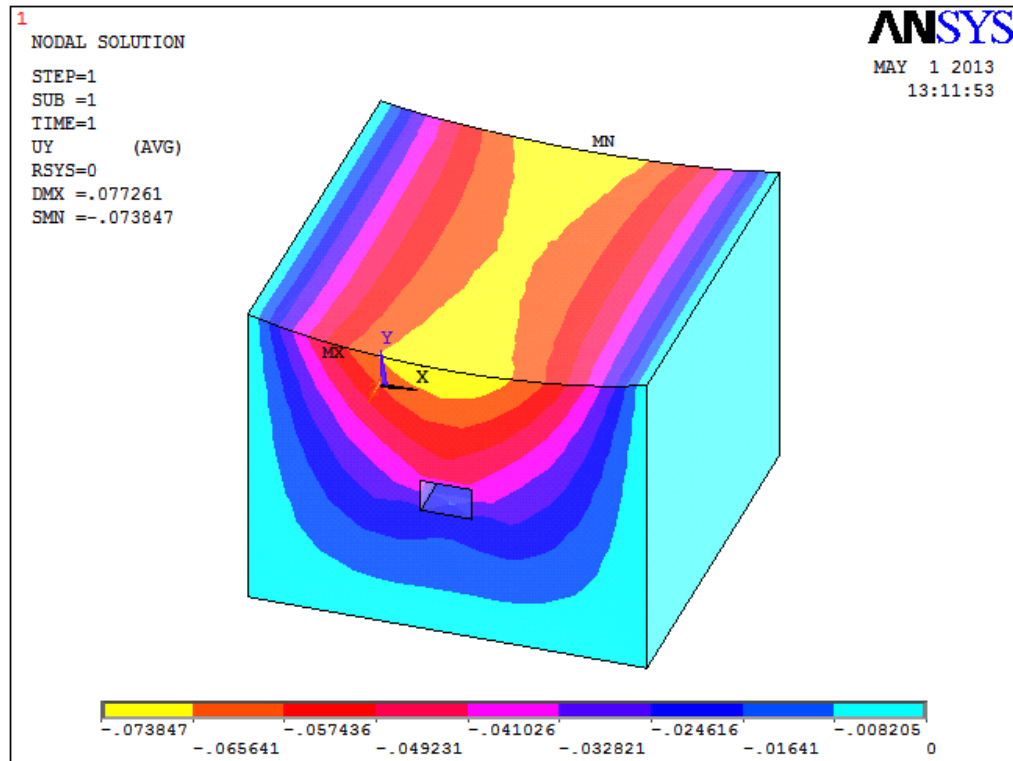


Figure 5.17: Deformation Contour plot of Gallery at Depth 90 m with Gallery width 3.6 m, Square Pillar (25 m x 25 m)

6. Stress contour plot of gallery at depth 100 m with Gallery width 4 m, square Pillar (25 m x 25 m) and pillar height 2.7 m. Maximum stress over the gallery was 3.72 MPa (figure 5.18).

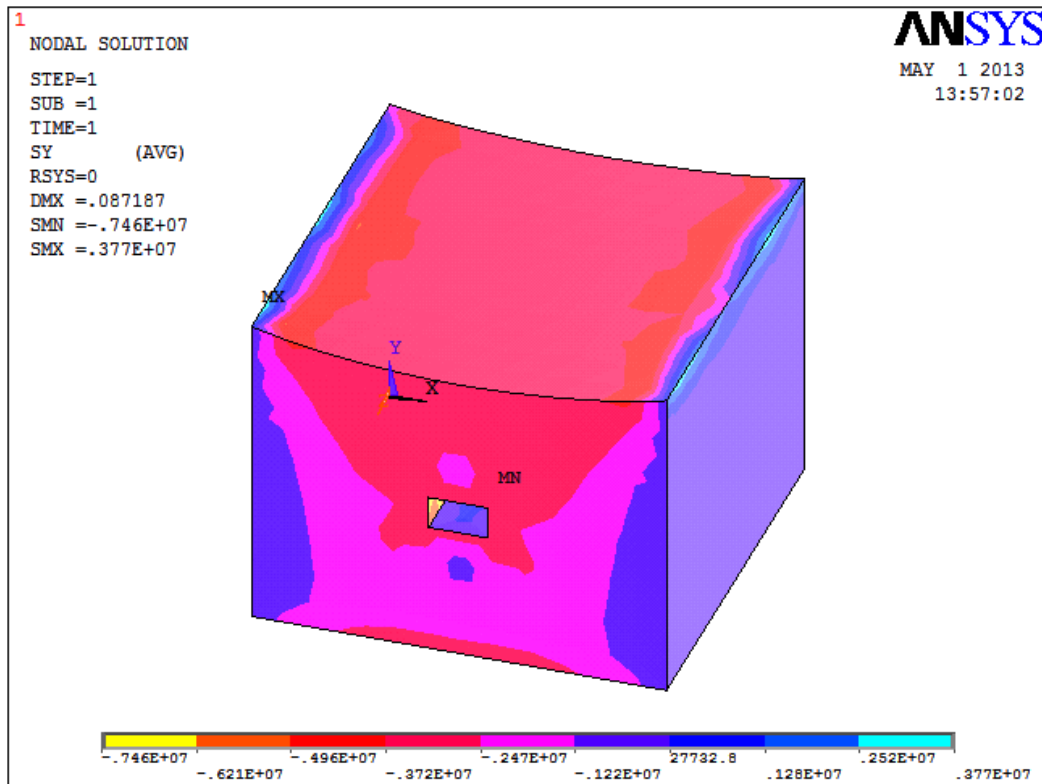


Figure 5.18: Stress contour plot of gallery at depth 100 m with gallery width 4 m, square Pillar (25 m x25 m)

7. Deformation contour plot of gallery at Depth 100 m with gallery width 4 m, Square Pillar (25 m x25 m), pillar height 2.7 m (figure5.19).Maximum sagging in the gallery observed was 0.0871 m (or 8.71 cm).

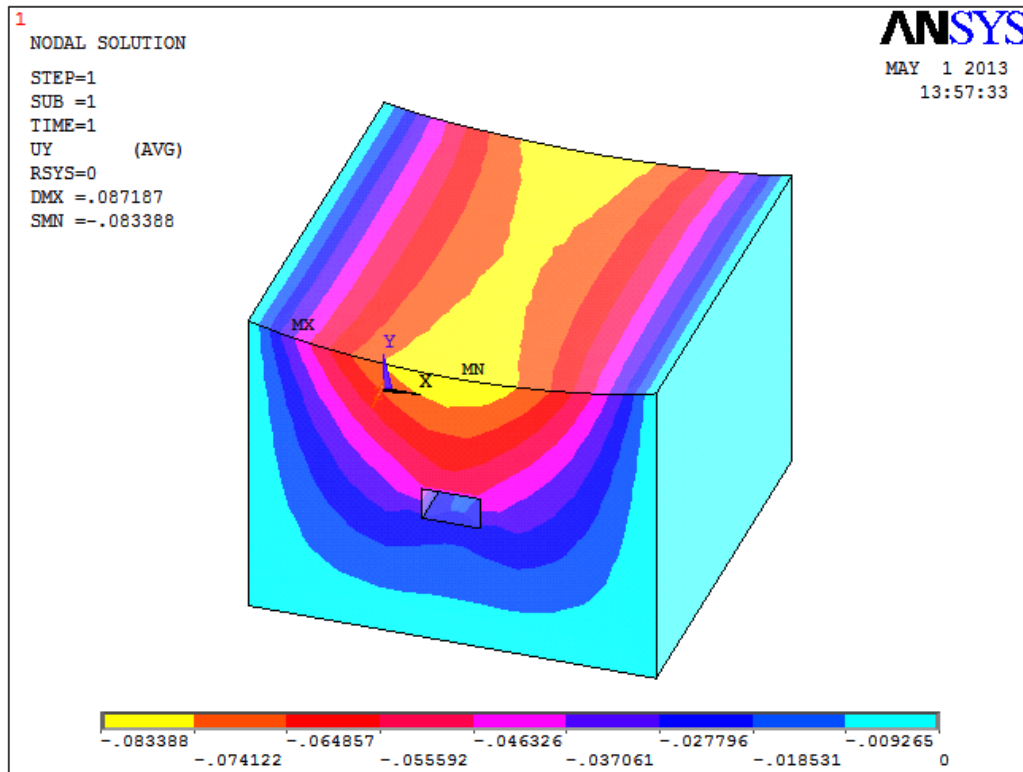


Figure 5.19: Deformation contour plot of gallery at depth 100 m with gallery width 4 m

## 5.2.2 Graphical Plot of Deformation and Stress for Result obtained

Analysis were carried out by varying the over burden loads on both pillar as well as on the room/entries. The pillar dimension considered was 25 m X 25 m X 2.7 m. It is observed that as the mining depth increases, stress and deformation in the pillar increases.

### 5.2.2.1 Effect of Depth cover on Deformation behavior in the Pillar

Maximum deformation at 60 m was 0.0091m (or 0.91cm) and at 120m it was 0.0173m (or 1.73 cm). It shows that as the depth increases deformation of the pillar also increases (figure 5.20 & Table 5.5). Deformation with depth of cover more or less follows a logarithmic function and can be used to find out approximate deformation at any depth. The mutual relation obtained is given by:

$$y = 0.0126\ln(x) - 0.0429 \text{ with } R^2 = 0.9796.$$

### 5.2.2.2 Effect of Depth cover on stress behavior over pillar

Maximum stress induced over the pillar was 3.20 MPa for depth cover of 120 m, and minimum was 1.64 MPa for 60 m depth. It means stress induced over the pillar increases with increase

indepth (figure 5.21 & Table 5.5). Stress developed over Pillar follow logarithmic relationship with depth cover. The mutual relation obtained is given by:

$$y = 2.3938\ln(x) - 8.2385 \text{ with } R^2 = 0.9781.$$

Table 5.5: Maximum deformation in the pillar and stress developed on the pillar with varying depth

Sl. no.	Depth (in meter)	Maximum deformation in pillar(in meter)	Stress developed on the pillar(in MPa)
1	60	0.0091	1.64
2	70	0.0105	1.91
3	80	0.0119	2.16
4	90	0.0133	2.42
5	100	0.0159	2.92
6	110	0.0165	3.05
7	120	0.0173	3.20

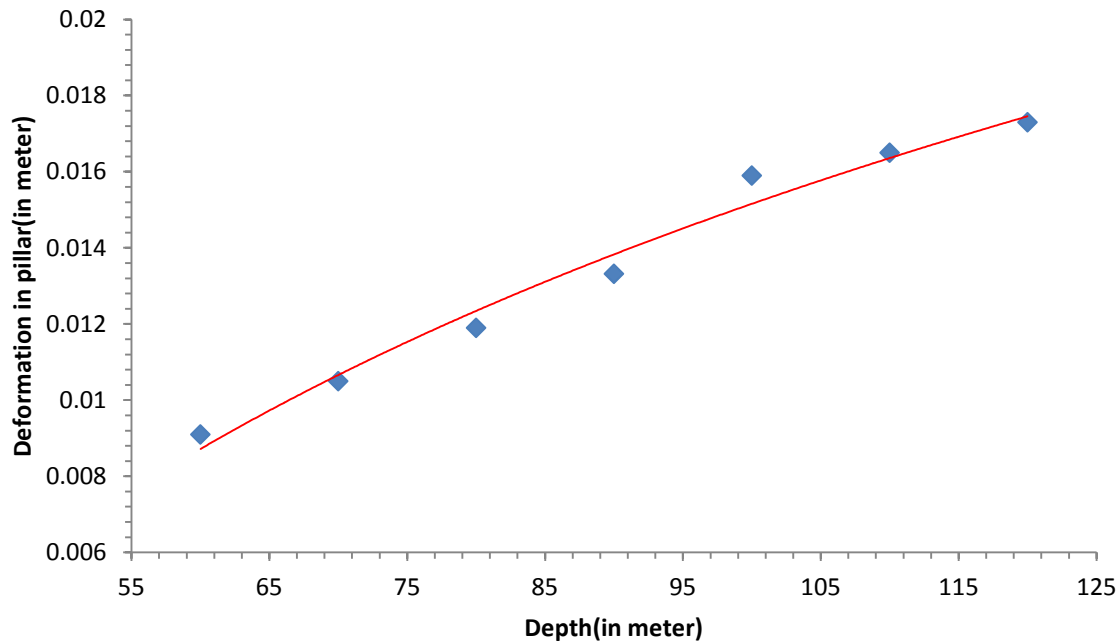


Figure 5.20: Depth verses deformation in pillar keeping pillar size constant (25 m X 25 m).

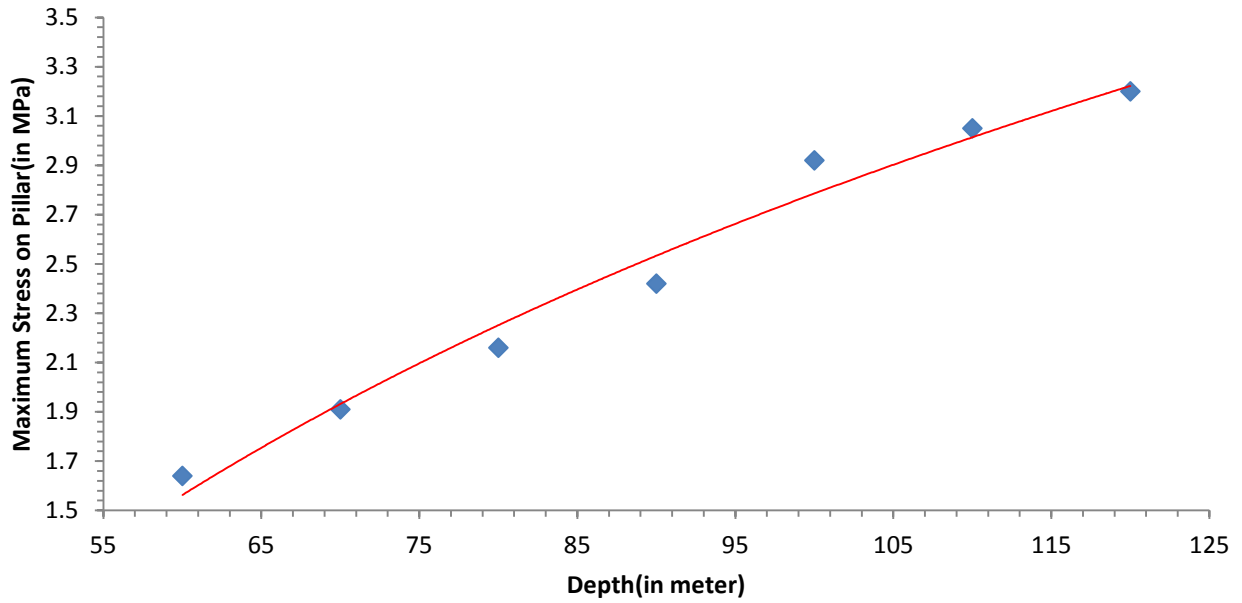


Figure 5.21: Depth verses maximum stress on the pillar keeping pillar size constant (25 m X 25 m X 2.7 m).

### 5.2.2.3 Effect of Pillar size on strain developed in the pillar

Maximum strain percentage developed in the pillar was 2.18 in the case of Pillar size of 21 m X 21 m and the minimum strain percentage was 2.02 for Pillar size of 25 m X 25 m. This shows that strain developed in the pillar increases with decrease in pillar size and would lead to the failure of pillar (figure 5.22 & table 5.6), if the deformation continues at a higher rate. Variation of strain with Pillar size more or less follows the polynomial relationship of degree 2. The mutual relation obtained is given by:

$$y = 0.0043x^2 - 0.2371x + 5.2706 \text{ with } R^2 = 0.9986$$

Table 5.6: Maximum deformation and strain developed over the pillar with varying pillar size keeping other parameters constant.

SL. NO.	Pillar size(in meter)	Deformation in pillar( $\Delta L$ )( in meter)	Strain Percentage in pillar( $\Delta L/L$ , where $L$ =pillar height)
1	21x21	0.0590	2.18
2	22x22	0.0576	2.13
3	23x23	0.0564	2.08
4	24x24	0.0554	2.05
5	25x25	0.0546	2.02



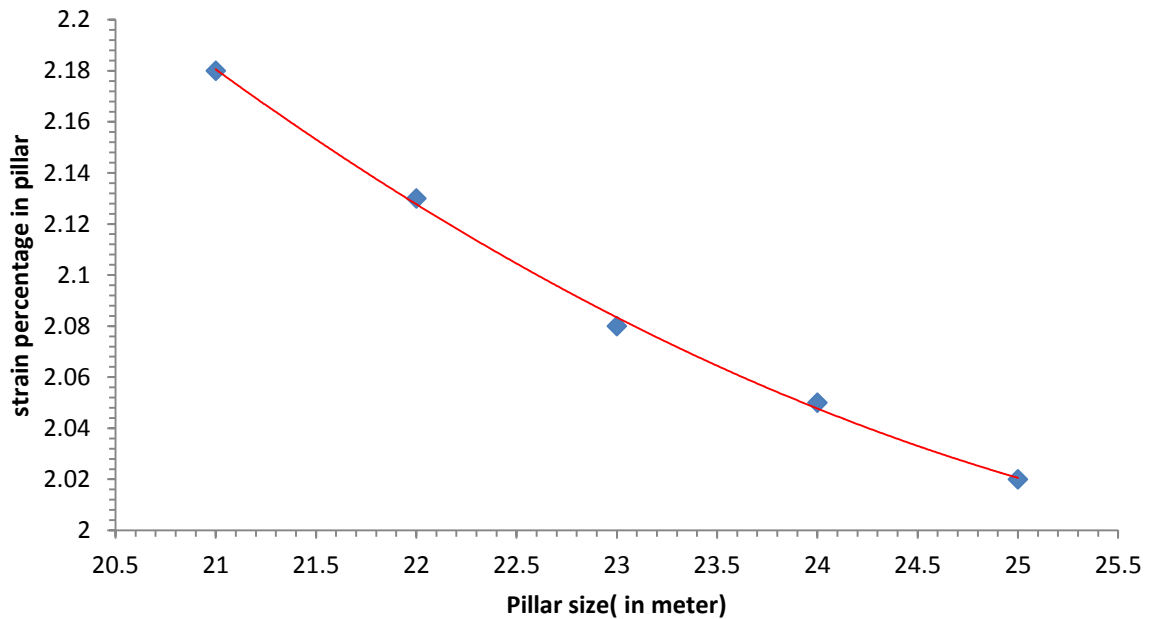


Figure 5.22: Pillar size verses strain developed in the pillar keeping depth 90 m constant.

#### 5.2.2.4 Effect of Gallery width on Sagging effect in the gallery

It is observed that as the gallery width increased sagging effect in gallery also increased. Maximum Sagging observed was 0.083 (Or 8.3 cm) in the case of 4.8 m gallery width and minimum in the case of 3m gallery width was 0.0747 (or 7.47 cm) without any external supports system (figure 5.23 & table 5.7). Sagging in the gallery follows the polynomial (degree 2) relationship with gallery width. The mutual relation obtained is given by:

$$y = 0.0003x^2 + 0.0019x + 0.0658 \text{ with } R^2 = 1.$$

#### 5.2.2.5 Effect of Gallery width on Stress Developed over the gallery

Gallery width has pronounced effect over the stress developed in the gallery. As the width of gallery increases, stress over the gallery also increases leading to sagging in the gallery (figure 5.24 & table 5.7). Minimum stress developed in the gallery for 3 m width was 2.17 MPa and the maximum was 3.87 MPa in the case of 4.8 m gallery width. The mutual relation obtained is given by:

$$y = -0.3472x^2 + 3.5983x - 5.451 \text{ with } R^2 = 0.9687.$$

Table 5.7: Maximum sagging in the gallery and maximum stress induced over the gallery with varying gallery width keeping other parameter constant.

SI. NO.	Gallery Width(in meter)	Sagging in gallery(in meter)	Maximum Stress developed in gallery(in MPa)
1	3	0.0747	2.17
2	3.6	0.0772	3.15
3	4.2	0.0800	3.39
4	4.8	0.0830	3.87

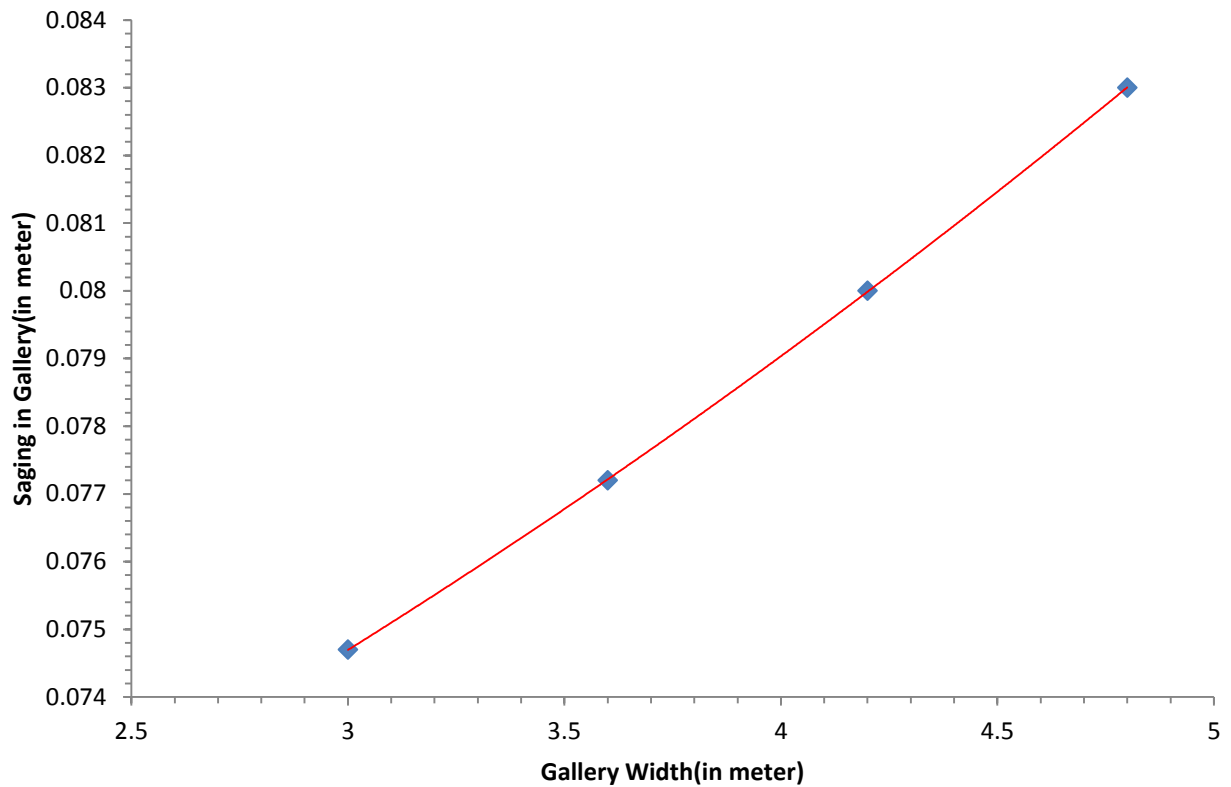


Figure 5.23: Gallery width verses sagging in gallery keeping pillar size (25 m X 25 m X 2.7 m) and depth 90 m constant

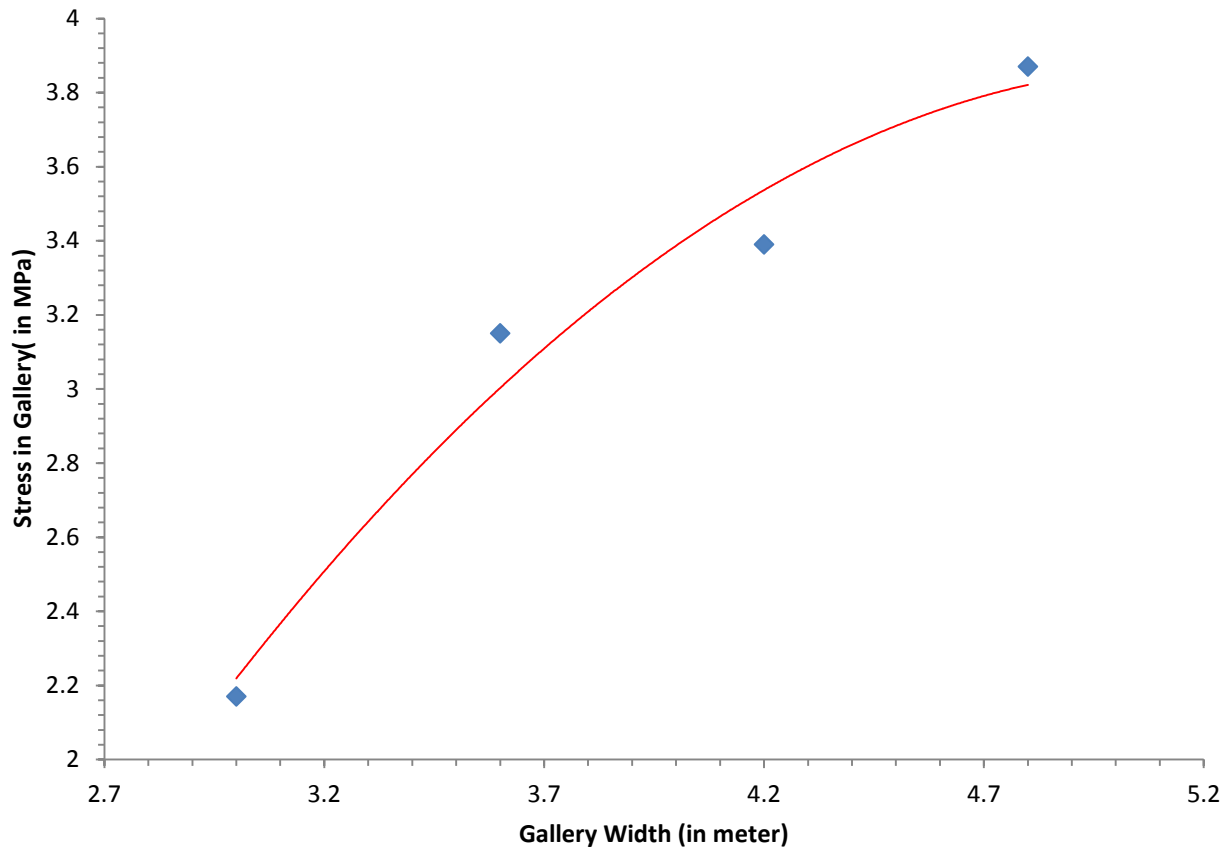


Figure 5.24: Gallery width verses stress in gallery keeping pillar size (25 m X 25 m X 2.7 m) and depth 90 m constant

#### 5.2.2.6 Effect of Depth cover on Sagging effect in the gallery

Effect of Depth cover on sagging in the gallery has more than that of gallery width. Sagging in the gallery is directly proportional to the depth cover (figure 5.25 & table 5.8). Maximum sagging observed was 0.0948 m (or 9.48 cm) at the depth of 110 m and minimum was 0.0541 m (or 5.41 cm) at the depth of 60 m. The mutual relation obtained is given by:

$$y = 0.0008x + 0.0057 \text{ with } R^2 = 0.9996.$$

### 5.2.2.7 Effect of Depth on stress Developed over the gallery

Maximum stress over the gallery at the depth of 110 m was 4.04 MPa and the minimum was 2.31 MPa for the depth 60 m. As the depth increases stress induced over the gallery is also increased (figure 5.26 & table 5.8). Stress over the gallery varies more or less linearly with depth. The mutual relation obtained is given by:

$$y = 0.0008x + 0.0057 \text{ with } R^2 = 0.9996.$$

Table 5.8: Maximum sagging and maximum stress developed over the gallery with varying depth cover keeping other parameters constant.

SI. NO.	Depth(in meter)	Sagging in gallery(in meter)	Maximum Stress Developed in gallery(in MPa)
1	60	0.0541	2.31
2	70	0.0627	2.67
3	80	0.0711	3.03
4	90	0.0792	3.38
5	100	0.0871	3.72
6	110	0.0948	4.04

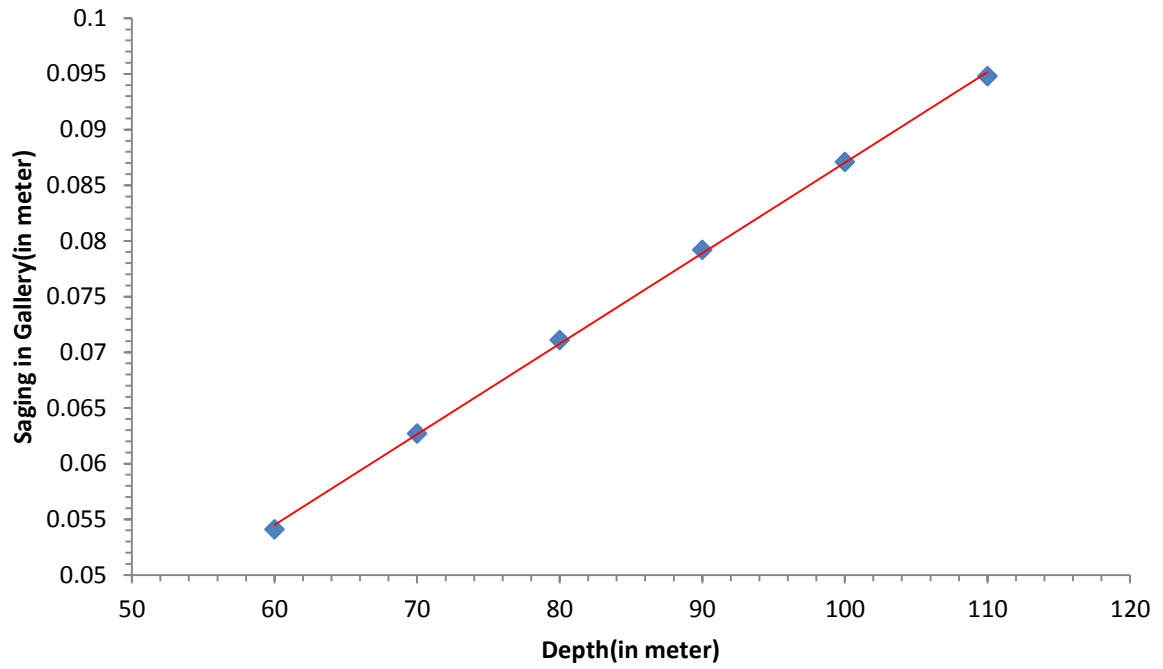


Figure 5.25: Depth verses sagging in gallery keeping gallery width 4 m constant.

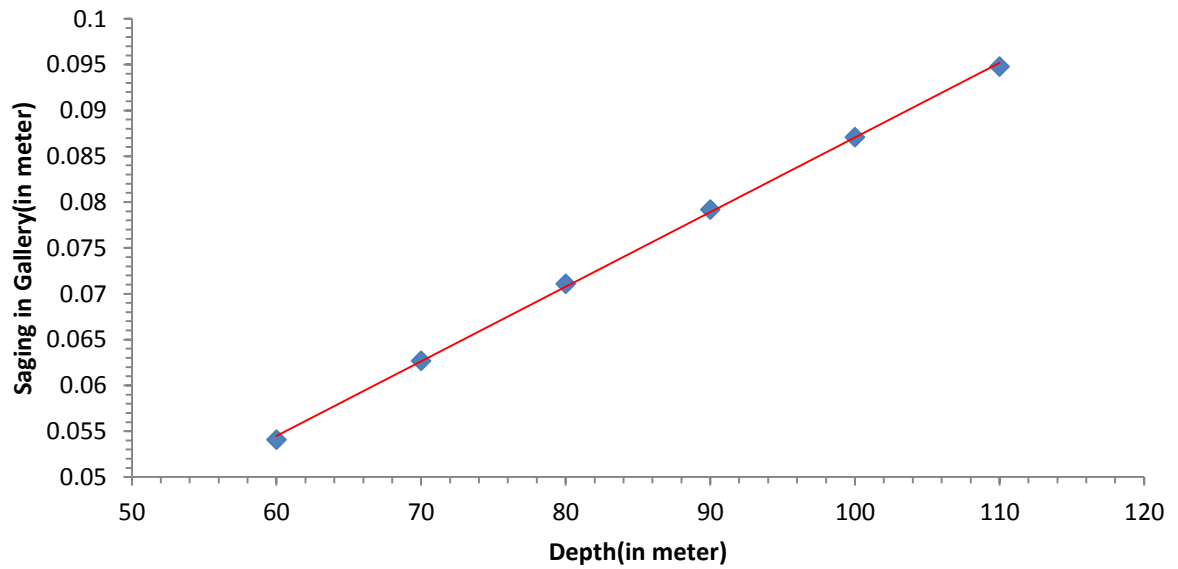


Figure 5.26: Depth verses stress in gallery keeping gallery width 4 m constant.

## **CHAPTER-6**

### **CONCLUSION AND RECOMMENDATION**

## 6.1 Conclusion

The investigation focused on evaluating coal pillar in a local mine. The following conclusions are drawn from the analyses. It is subdivided into three parts to include the data from the field visits, safety factor analyses and stress-strain evaluation from numerical modeling

### A. Case Study Mine:

- Bord and Pillar method of mining with DGMS guidelines are followed with square size pillars.
- The maximum vertical stress over the pillar top was 3.12 MPa at 120 m depth and minimum was 1.56 MPa at 60 m depth.
- Horizontal stress ( $\sigma_h$ ) determined is 0.369, which is very low as compared to the vertical stress.

### B. Safety Factor analysis:

- Various approaches like CMRI, Obert-Duvall, Bieniawski were used in estimating safety factor with varying mining parameters (i.e. depth, pillar dimension etc).
- Variation in the Safety factors obtained using CMRI, Bieniawski and Obert-Duvall approaches were analyzed. Maximum and minimum safety factor in CMRI approach was 3.1 and 2.54, maximum and minimum safety factor in Obert-Duvall approach was 2.72 and 1.651, maximum and minimum safety factor in Bieniawski approach was 3.737 and 2.322 (figure 5.1).
- The extraction percentage varies from 29.3 to 25.2 (figure 5.2). Maximum extraction percentage can be achieved by optimizing pillar dimension and gallery width.

### C. Stress, deformation and sagging Analysis:

Maximum stress induced over the pillar and the deformation in the pillar with varying various parameters like depth, pillar size, Gallery width using ANSYS was estimated. Sagging effect in the gallery and the stress over the gallery was also estimated with varying gallery width and depth cover. Depending on the results obtained from the numerical modeling, following conclusions were drawn:

- With increase in the depth cover, deformation in the Pillar and stress developed over the pillar kept on increasing (figure 5.20 & 5.21). Maximum and minimum deformation observed was 17.3 mm and 9.1 mm.
- As the pillar size decreased, strain developed in the pillar is also increased (figure 5.22). Maximum strain developed in the pillar observed was 2.18% and minimum was 2.08%.
- Sagging in the Gallery and stress induced over the Gallery increases as the gallery width and the depth cover increases (figure 5.23, 5.24, 5.25 & 5.26). Maximum and minimum sagging observed in the gallery was 83 mm and 74.7 mm respectively. While the maximum and minimum stress induced over the gallery was 3.87 MPa and 2.17 MPa respectively.

## **6.2 Recommendation**

- More coal samples and pillar specimen should be included to provide a more reliable result.
- Seam inclination should be considered to give a better realistic analysis.
- Numerical modeling should be carried out incorporating roof, floor properties as well as coal pillar characteristics.



## REFERENCES

1. Mark, C., 1981-2006, The evolution of intelligent coal pillar design, P.P: 2-4.
2. Peng, S. S. Coal mine ground control. New York, John Wiley & Sons. 1978. pp. 181-182.
3. Wagner, H., (1980). Pillar design in coal mines. J.S. Afr. Min. Metal., V80, pp. 37- 45.
4. Bieniawski, Z.T., 1992, Ground Control, Chapter in Mining Engineering Handbook, SME, P.P: 897-937.
5. Singh, R.D., Principles And Practices Of Modern Coal Mining, New Age International Limited Publishers, 1st Edition, 2005, Chapter 6, pp. 156-180.
6. Bieniawski, Z. T., 1984, Rock Mechanics Design in Mining and Tunneling, A.A.Balkema.
7. Bieniawski, Z.T., (1968). The effects of specimen size on the compressive strength of coal. Int. J. Rock Mech. Min Sci. Vol. 5, pp.325-335.
8. Das, M N, 1986. Influence of width to height ratio on post-failure behavior of coal, International Journal of Mining and Geological Engineering, 4:79-87.
9. Sheorey P. R. Pillar strength considering in situ stresses. Workshop on Coal Pillar Mechanics and Design, pp. 122-127. Santa Fe, USBM IC 9315 (1992).
10. Roberts D.P., Van der Merwe J.N., Canbulat EJ Sellers I., and Coetzer S., "Development of a method to estimate coal pillar loading", Report No : 2001-0651, September 2002.
11. Shrivastva, B.K. & Jaiswal, Ashok, Numerical simulation of coal pillar strength (2009), International journal rock mechanics and mining sciences 46 (2009) 779-788, Elsevier Ltd.
12. Y. Nakasone and S. Yoshimoto, Engineering Analysis With ANSYS Software (2006), first edition , Oxford, London.
13. Kushwaha, A, Shorey P.R. , Mohan, G.M., Numerical estimation pillar strength in coal mine (2001), International journal rock mechanics and mining sciences 38 (2001) 1185-1192, Elsevier Ltd.
14. <http://www.scribd.com/doc/127177039/Ansys-Manual-pdf>
15. [http://www.ansys.stuba.sk/html/guide\\_55/g-bas/GBAS1.htm](http://www.ansys.stuba.sk/html/guide_55/g-bas/GBAS1.htm)